J Mater Sci (2012) 47:68–92
DOI 10.1007/s10853-011-5926-5

ANNIVERSARY REVIEW

The diversity of combustion synthesis processing: a review

K. Morsi

Received: 11 July 2011 / Accepted: 31 August 2011 / Published online: 23 September 2011

Abstract The harnessing of heat emanating from powder-based exothermic reactions to produce advanced materials has been around for many decades, and is manifested in the process of combustion synthesis (CS). A plethora of work has been published on the topic covering fundamental aspects of the process for a large number of material systems. Over time, CS has been combined with other processes and effects to potentially improve on conventionally produced CS products and alleviate some of the inherent disadvantages of CS. This article discusses processing aspects of CS, and provides a review of CS-related hybrid processes with the intent to exemplify the diversity of CS processing. Approaches such as reactant microstructural design, reactive bulk deformation/compaction processes, reactive casting, laser-assisted CS, activation techniques (field/current, mechanical, microwave), and unconventional heat treatments are discussed together with other methods.

Abbreviations

AC	Alternating current
BPR	Ball-to-powder weight ratio
CAD	Computer aided design
CS	Combustion synthesis
CS-SPS	Combustion synthesis-spark plasma sintering
DC	Direct current
ECAE	Equal channel angular extrusion
ECAP	Equal channel angular pressing
FACS	Field-activated combustion synthesis
FF-MGE	Free-fall microgravity environment
HA	Hydroxyappatite
HERS	Hot extrusion reaction synthesis
HPSHS	High pressure self-propagating high temperature synthesis
MA	Mechanical alloying/activation
MA2P	Mechanically activated annealing process
MACS	Microwave-assisted/activated combustion synthesis
MASHS	Mechanically activated self-propagating high temperature synthesis
MARES	Mechanically activated reactive extrusion synthesis
MARFOS	Mechanically activated reactive forging synthesis
MSR	Mechanically induced self-propagating reaction
ODS	Oxide dispersion strengthened
PF-MGE	Plane parabolic flight microgravity environment
SEM	Scanning electron microscope
SHS	Self-propagating high temperature synthesis
SLS	Selective laser sintering
SPS	Spark plasma sintering
SRS	Shock-induced reaction synthesis
TACS	Thermally activated combustion synthesis

K. Morsi (✉)
Department of Mechanical Engineering, San Diego State University, 5500 Campanile Drive, San Diego, CA92182, USA
e-mail: kmorsi@mail.sdsu.edu

Introduction

As the world becomes more energy-conscious, the harnessing of heat produced from an exothermic reaction between constituent powders to produce advanced materials may be viewed as a step in right direction. This is the case for the combustion synthesis (CS) process which is appropriately often referred to as one with a low thermal budget. The heat emanating from reactions between

Fig. 1 Examples of combustion synthesis-related level-1 hybrid processes and effects

reactant powders can indeed alone raise the temperature of a powder compact by many hundreds of degrees which can facilitate both product formation and sintering in relatively short times. The theory of the self-propagating mode of CS was published by Booth in 1953 [1, 2]. Merzhanov and Borovinskaya [3] recently discussed the production and technological applications of the process and its developmental history, where its development was divided into three periods beginning with the Chernogolovka period, followed by Soviet period and finally a worldwide period. As such, from the 1980s onwards; the US and other countries have taken a progressively active role in CS research [2]. A plethora of material systems and composites have been formed using CS, including titanium carbide [4], nickel aluminides [5], nitrides [6], silicides [7–9], cermets [10, 11], functionally graded materials [12], and recently even nanotube reinforced nickel aluminide [13]. Over the past 25 years many valuable review articles have been published on the topic [3, 14–32], covering experimental and modeling aspects of the CS, its application to nanostructural systems, nanocomposites, perovskites and spinels, electromagnetic radiation effects both intrinsically generated within the process and externally applied to the process, TiC–TiB_2 composites, thermal, mechanical, and mechanical–thermal activation of in situ aluminum-based composites, production and technological applications, and environmental applications of the process. The reaction synthesis processing of Ni–Al intermetallics has also been reviewed by the author [33].

Recent developments and new approaches within the field of CS have demonstrated its high level of diversity. Figure 1 shows examples of CS and CS-related processes and effects. The present author believes the processes in the figure can be classified as level-1 hybrid processes, such as reactive extrusion, reactive infiltration, mechanically activated SHS (MASHS), where CS has been combined with one other "basic" process or effect. It should be noted that in the figure it is implied that the word extrusion in reactive extrusion encompasses all forms of extrusion, such as equal channel angular extrusion, hydrostatic extrusion, direct, and indirect extrusion, etc., within the self propagating and thermal explosion modes of ignition of the reactant powders. Likewise pressing includes uniaxial, isostatic, pseudo-isostatic, high pressure, etc. The figure does not include level-2 and higher-level hybrid processes, which have also been adopted in CS and will be discussed in this article. These would include processes such as mechanically activated reactive extrusion synthesis, or reactive spark plasma extrusion (i.e., level-2 hybrid processes). Understandably, for example if mechanical activation is combined with current activation and extrusion for reactive systems, this would represent a level-3 hybrid process, and so on. This type of progression exemplifies the diversity of CS processing and its effective single and

Table 1 Examples of level-1, level-2, and level-3 hybrid processes with their advantages and disadvantages

Process	Additional effect/process	Advantages	Disadvantages
Level-1 hybrid process			
Reactive/SHS extrusion	Extrusion	High degree of consolidation, rapid shaping, possibility of re-crystallized/refined microstructures (for extrusion, forging and rolling)	Added expense in pressure application and tooling. Defect formation/inhomogeneous microstructures if timing of pressure application is not optimized
Reactive/combustion forging	Forging		
Reactive/SHS rolling	Rolling		
Reactive pressing	Pressing		
Reactive casting (non-centrifugal)	Casting	Energy Savings over conventional melting practices in casting processes	Pre-curser powders used (e.g. in SHS casting) may be relatively expensive, and possible formation gas porosity if not addressed
Laser-assisted combustion synthesis (SHS–SLS)	Laser interaction	Production of intricate shapes, rapid prototyping	Can generate highly porous and inhomogeneous materials
Microwave activated/assisted combustion synthesis	Microwave activation	Realizing SHS processing for previously unfavorable powder systems. Can combine reactive processing with regular microwave sintering in one cycle	Equipment/setup expense
Mechanically activated SHS	Mechanical activation	Realizing SHS processing for previously unfavorable powder systems, reduced ignition temperatures, increased wave velocities, ability to produce nanostructured products	Added separate MA processing step which can be in hours, potential for powder contamination during MA step, High levels of porosity in final product
Level-2 hybrid process			
Mechanically activated reactive extrusion synthesis	Mechanical activation + extrusion	High degree of product consolidation, product shaping with good dimensional control, nano/refined microstructures	Added MA step and added expense in pressure application and tooling. For NiTi processing, microstructural in-homogeneities, requiring further heat treatments
Mechanically activated reactive forging synthesis	Mechanical activation + forging		
Level-3 hybrid process			
Mechanically activated spark plasma sintering	Mechanical activation + pressing + current activation	Highly consolidated products, ability to form nanostructured products	Added expense in pressure and power application and tooling. Possibility of not generating a single phase product, although increased heating rate has been shown to avoid this for certain systems

multi-level hybridization with other processes and effects to potentially eliminate its shortcomings, and present added advantages and possibilities. Table 1 provides examples of some of these processes and their hybridization level with possible advantages and disadvantages. The material systems investigated so far are numerous and also constantly growing, covering more and more systems suitable for an extensive array of applications.

As such, this article briefly discusses processing aspects of CS, and provides a review of CS-related hybrid processes. Due to the extremely large number of published papers on the subject, this review is not intended to cover all the publications in the area; however it aims to display and exemplify the diversity of CS processing and its amenability to hybridization with other processes and effects. Although the article is inclined more towards the

CS of intermetallics, discussions on the CS of some ceramics and composites are also included, covering selected research conducted mainly within the past 30 years. However, the article excludes CS techniques for the production of powder. Influences of electric field/current, mechanical and microwave activation are discussed, together with other emerging hybrid processes such as laser-assisted CS, reactive extrusion, and reactive forging, among others. Moreover, the influences of new microstructural designs and heat treatments on the developed product(s) are also discussed.

Processing aspects of combustion synthesis

CS processing parameters and observed phenomena

Combustion synthesis (or reaction synthesis) of powders involves the reaction of elemental or otherwise reactive powder constituents to form the intended product phase(s). The process is exothermic in nature whereby high temperatures are generated specifically due to the enthalpy of formation of the product(s). The process encompasses two modes of ignition that define other sub-processes. One of these sub-processes is self-propagating high temperature synthesis (SHS) (although CS and SHS have also been used interchangeably) in which a reactant powder compact is ignited at one end, forcing a local reaction that then travels as a reaction wave along the whole compact consuming the reactants and forming the product(s) in its wake. The reaction once initiated becomes self-sustaining; the actual initiation can be triggered by a resistively heated coil, laser heating as well as other different techniques which have been previously reviewed by Barzykin [34]. In SHS the whole compact may initially be at room temperature or pre-heated (typically carried out for reactions with low enthalpies of product formation) to a uniform temperature prior to SHS ignition.

The other sub-process is *volumetric combustion* where the whole compact is heated uniformly to the ignition temperature to provide for a simultaneous and uniform reaction all over the compact. Understandably, it has been also termed *simultaneous combustion*, in addition to *thermal explosion*. In most cases there is a one-time significant amount of energy that is released due to the reaction.

Many factors can influence the successful implementation of CS, and therefore need to be carefully considered. These include particle size, green density, environment/atmosphere, heating rate, ignition temperature, pre-heating temperature, mechanical activation, current/field activation, applied pressure, and pre-ignition heat treatments. An important gage that is often reported in these types of reactions is the combustion temperature (T_c), which is simply defined as the maximum temperature achieved experimentally during the reaction. This temperature can be also theoretically predicted through thermodynamic analysis given enthalpy of formation and heat capacity data. In this case the theoretically predicted maximum temperature is termed the adiabatic temperature (T_{ad}). Depending on the product enthalpy of formation, the adiabatic temperature can be below, equal to or above the product melting point, T_m, and is defined according to the following equations [2]:

$$X(s) + Y(s) \rightarrow XY(s) \tag{1}$$

If $T_{ad} < T_m$

$$\Delta H^o_{f298} = \int_{298}^{T_{ad}} C_{p(s)} dT \tag{2}$$

If $T_{ad} = T_m$

$$\Delta H^o_{f298} = \int_{298}^{T_m} C_{p(s)} dT + v\Delta H_m \tag{3}$$

If $T_{ad} > T_m$

$$\Delta H^o_{f298} = \int_{298}^{T_m} C_{p(s)} dT + \Delta H_m + \int_{T_m}^{T_{ad}} C_{p(l)} dT \tag{4}$$

where ΔH^o_{f298} = enthalpy of formation of compound XY at 298 K, $C_{p(s)}$ and $C_{p(l)}$ = heat capacity in the solid and liquid states, respectively, of the product XY (which are temperature dependent), ΔH_m is the enthalpy of fusion of product XY, and v is the fraction of molten XY product (from 0 to 1).

The word adiabatic refers to an assumption of zero heat loss from the compact, from the time of ignition to the maximum temperature achieved. This is somewhat justified only in very rapid reactions that take the compact to the maximum temperature leaving very little time for heat loss to the surroundings. It is understandable that the experimentally determined combustion temperature can in fact fall below the adiabatically predicted temperature due to incomplete reactions and failure to achieve true adiabatic conditions. However, in some other cases the combustion temperature can in fact exceed the adiabatic temperature. An example of this is if unintentionally oxidation occurs and consequently a supplemental amount of energy is added to the system. Nevertheless, knowing the maximum temperature that occurs during the reaction can be very important in revealing the state of the material during the reaction and also predicting whether a material would even undergo SHS or not. For example, it has been empirically proposed that as long as the T_{ad} is equal to or exceeds

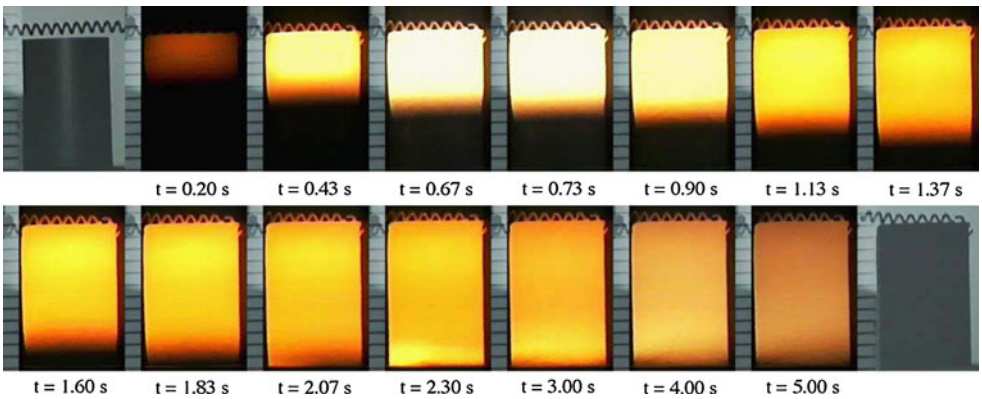

Fig. 2 Wave propagation in the SHS of Ni_3Al [37]

1,800 K then SHS reactions can be sustainable [35]. Alternatively, Munir et al. [2, 36] suggested that material systems with $\Delta H^{o}_{f298}/C_{p298} \leq 2.0 \times 10^{3}$would not undergo SHS in the absence of external heating.

In SHS, a successful propagating reaction wave is normally referred to as "stable", in other words the wave travels at constant velocity. Velocities in the range of 6×10^{-4}–2.5×10^{-1} m/s have been typically reported for a variety of cases [2]. Figure 2 from recent work shows wave propagation during the SHS of Ni_3Al [37].

If the reaction kinetics, thermodynamics and heat transfer characteristics are not favorable, then such stability can be lost. In this case the wave can take different forms. It can either alternate between high and low velocities, which is termed "oscillatory" or follow a kind of a spiral path, termed "Spin". Both of these are within an unstable categorization of wave propagation. It is understandable that an even more drastic situation would be eventually the total extinction of the wave all together. Approaches that are used to avoid such negative events include pre-heating the powder compact, controlling reactant powder composition (and therefore enthalpy of product formation), powder size, and other forms of activation, such as mechanical activation as demonstrated for Cu_3Si [38], or electric field activation as demonstrated for the titanium aluminides [39] among other systems (these will be discussed later). Preheating should ultimately lead to an increased combustion temperature and wave velocity. It should be mentioned; that although compact pre-heating can lead to an increase in wave velocity, this is not always the case. For example, work by Sohn and Wang [40], on the SHS of Al_3Ti and Ni_3Al, has shown that pre-heating the compact does initially lead to an increase in the wave velocity, however only up to some given temperature, above which a decline in wave velocity is observed (in addition to an accompanied reduction in combustion temperature). This was attributed to the formation of low temperature reaction products by solid-state diffusion between the elemental powders which hindered aluminum spreading during SHS.

The particle size of reactants can also play an important role in CS, for example, in field-activated studies; a particle size limit can exist above which field-activated combustion synthesis (FACS) is not possible. In conventional SHS studies, particle size has been shown to have an inverse relation with wave velocity, with the highest velocities achieved at the smallest particle sizes [25]. Although this is generally true, as the particle size is reduced other factors need also to be taken into account. This is especially true for nanoscale powders where a considerable fraction of the particle volume is occupied by surface oxides, and physical properties of the particle can be substantially different from the customary larger particles even of the same material. Recent SHS work on the Ni–Al system has shown that when aluminum particle size was reduced to 25 nm, time-to SHS ignition using a laser source was reduced (primarily due to the reduced aluminum melting point at the nanoscale) and a homogeneous reaction front was achieved (due to the absence of large voids that allow convective flame spreading), despite a considerably low initial green density of ~30% [41]. However, the expected increase in wave velocity was not achieved, primarily due to a buffering (diluting) effect of the substantial surface oxides present on the nanoscale aluminum (~46%). It is well known that for Ni–Al systems ignition typically occurs around the eutectic temperature of 640 °C [33]. The ignition temperature has been reported to be reduced by hundreds of degrees, to 286 °C when nanoscale aluminum was used [41]. Ignition temperature in other material systems such as Ti–Al have also been found to be heating rate dependent in thermal explosion type experiments using a high frequency vacuum induction furnace [42], to the point where ignition actually occurs at temperatures that exceed the melting point of aluminum, i.e., up to 850 °C at a heating rate of 300 °C/min. Fu et al. [43] reported an ignition temperature of ~900 °C when using heating rates between 1,200 and 1,500 °C/min (achieved with the use of induction heating). Although it shows a much lower dependence of ignition temperature on heating rate beyond 300 °C, the ignition temperature is still, however, above that of the melting

point of aluminum, giving rise to an initial reaction between molten aluminum and solid titanium to form Al_3Ti. Ignition temperatures above the melting point of aluminum have also been reported for Al_3Nb [44].

While a large number of studies have investigated CS under normal gravity, some have carried it out under microgravity conditions. Interestingly, it has been shown that microgravitational effects can influence SHS if a liquid or gas is present during the reaction. For example, wave velocities have been observed to be lower for SHS reactions conducted under microgravity conditions as opposed to terrestrial conditions [45], increased pore content in the reaction zone has been suggested as limiting the apparent thermal conductivity. For artificial or normal gravity conditions, it has been shown that the orientation/direction of wave velocity vector in relation to the gravity vector can influence SHS characteristics when a liquid is present [46]. Hence the gravitational force can act to compress or expand the combustion zone during SHS depending on the orientation relative to the propagating wave. Research by Odawara [47], using free-fall microgravity environment (FF-MGE) generating 10^{-4} g ($g = 9.81$ m/s^2) and plane parabolic flight microgravity environment (PF-MGE) generating 10^{-2} g has shown a reduction in wave velocity under MGE compared to ground. Even more interesting is the finding that Al–AlB_{12} wetting on TiB_2 is remarkably enhanced with degree of microgravity from FF-MGE to PF-MGE. Both PF-MGE and FF-MGE are limited by the small duration in which microgravity conditions are established, and hence can restrict the span of SHS stages that can be evaluated. This time limitation was avoided by Merzhanov [46] by conducting SHS experiments on a space station. A number of benefits of SHS reactions in this context have been identified by Sytschev and Merzhanov [48], which include processing of materials with high porosity, production of luminous radiation and thermal energy, and in-space repair and even fabrication. Recently, Zanotti et al. [49] reported an increase in the combustion temperature under microgravity conditions compared with normal gravity. Since in both cases similar phases were formed, the increase in combustion temperature was attributed to reduced heat losses under microgravity conditions, due to the holding of the liquid phase by capillary force and the avoidance of being pulled away by gravity leading to improved reactant contact. This finding is contrary to work by Locci et al. [45] in which they did not observe any significant change in combustion temperature by going from terrestrial to microgravity conditions.

Magnetic fields have also been found to significantly affect the SHS processing in terms of structure and products of powder mixtures that contain ferromagnetic constituents [50]. While the application of an external field has been shown for some time to influence CS processing, mechanisms by which SHS reactions can on their own 'intrinsically' produce electromagnetic radiation sounds at first somewhat surprising. However, this phenomenon has been recently discussed in an review by Filimonov and Kidin [51] in which they discuss both influences of internally generated electromagnetic radiation during CS and the influence of electromagnetic external field on CS.

Porosity and CS

A major problem that has plagued the CS process has been the generation of unwanted product porosity. The sources of this porosity have been previously well documented [2, 19, 52], and include the sudden evaporation of low boiling point impurities and adsorbed moisture on the surfaces of the powder (hence powder or green compact degassing procedures are customarily adopted prior to actual CS), in some cases at low heating rates the unbalanced diffusivities between different elemental powders can give rise to Kirkendall porosity following solid-state inter-diffusion (which is also often accompanied by the formation of unwanted phases and compact swelling), porosity carried forward from the green compact and porosity brought upon by solidification shrinkage (occurs if the product melts at the combustion temperature as in the case of NiAl in the absence of melt replenishment [52]]. Atmosphere has also been reported to affect porosity, such that CS under vacuum has been reported to give best results in the absence of externally applied pressure (this is also a typical observation in conventional "non-reactive" solid-state sintering studies) for nickel aluminides [53]. Of prime importance is also an "intrinsic" type of porosity generated due to the inherent differences in molar volumes between products and reactants. This alone can account for more than 10% in certain systems [19]. In systems where a liquid phase is formed and spreads, large pores (which can be difficult to remove) may be left behind at the prior large particle site of the molten phases [54]. To combat this problem of porosity, careful selection of powder size, environment, microstructural, and process design, in addition to the application of pressure have been adopted as solutions.

While the presence of porosity is often looked upon negatively, in certain cases controlled levels of porosity are in fact desired, such as when the objective is to manufacture filters or foams, with recent examples including the production of porous $MoSi_2$ and TiC via CS [55, 56], and metallic foams [57], respectively. Porous Perovskite catalysts have also been recently produced [58], in addition to the processing of porous biocompatible materials such as titanium nickelides using SHS [59], whereby pores can be used to accommodate bone in-growth.

Apart from the use of space fillers, there have been a number of approaches adopted within the field of CS with

the intent to form porous materials. As previously mentioned, one of the reasons for porosity generation in CS has been the volatization of adsorbed species from powder surfaces, Kobashi et al. [60], used these effects together with B_4C as an exothermic agent (which reacts with extra Ti added to allow the highly exothermic reaction, $3Ti + B_4C \rightarrow 2TiB_2 + TiC$) to produce Al–Ti and Al_3Ti/Al composites, starting with elemental powder. Successful foaming in the absence of B_4C was found to be sensitive to Al/Ti ratios such that ratios less than 3 did not achieve successful foaming. Successful foaming for a wide range of Al/Ti was possible with the aid of B_4C and Al/Ti ratios in excess of 5 resulted in more circular and spatially homogeneous pores. In a separate study, Hunt et al. [57] used nanoreactant powder to produce foamed NiAl up to 80% porosity. Here a gasifying agent was used, in the form of a perflourotetradecanoic acid ($C_{13}F_{27}COOH$) coat on nanoparticles of aluminum produced by self-assembly (The coat was included also to pacify the nanoaluminum, which can otherwise be pyrophoric). These nanoparticles were mixed with nano-nickel and micro-scale aluminum powder. The use of nanoparticles of aluminum reduced ignition times by two orders of magnitudes at a 2.24 wt% loading. The increase in gasifying agent content from 0 to 14 wt% increased porosity correspondingly from 10 to 80 wt%.

In another approach, the use of pre-combustion heat treatments has recently been investigated to produce porous materials following CS processing. It is well known that for nickel aluminides, low heating rates can give rise to the formation of aluminum-rich intermetallics such as Al_3Ni and Al_3Ni_2 (accompanied by Kirkendall porosity) produced through solid-state interdiffusion (at temperatures lower than the first eutectic (ignition) temperature). This can give rise to inhomogeneous product microstructures when aluminum is not a major phase, due to consumption of aluminum prior to reaching the ignition temperature, and a reduction in the combustion temperature. These phases have often been looked upon in a negative light, and higher heating rates have typically been recommended to minimize/avoid them. However, these same phases where grown intentionally in a recent study by Morsi et al. [61] through a pre-combustion synthesis heat treatment for the production of NiAl. In the NiAl system, in the thermal explosion mode of CS of Ni + Al, excessive heat of formation tends to melt the NiAl product. The pre-formation of these aluminum-rich phases by controlled heat treatment at 410 °C before heating up to the ignition temperature were found not only to act as an effective dilutant, that buffers the reaction (discussed in the next section), but also become totally consumed during the reaction leaving only porous 'single' phase NiAl (~60% porosity). Dong et al. [62], further examined the effect of green compact heat treatment (at 575 °C) on the developed open pore content, volume change and maximum pore size. Following heat treatment, compacts were sintered at 1,000 °C, and it was found that the maximum pore size decreases with increase in green compact heat treatment duration. In a separate study, Dong et al. [63] examined the effect of aluminum content (Ni–10 wt% Al to Ni–40 wt% Al) on pore formation of Ni–Al intermetallics. Here a preheat temperature of 600 °C for 4 h was used followed by sintering at 1,100 °C for 3 h. The volume expansion, maximum pore size and permeability were all found to increase with increase in aluminum content. A maximum open porosity of ~55% for sintered samples was obtained at the highest investigated aluminum content [63].

Interestingly, gravity has also been shown to influence the pore size, pore distribution and content. In a study by Guojian et al. [64] using the Ti + C reaction as a chemical oven under gravity and microgravity environments, observed less, finer and uniformly distributed porosity within the TiC product under microgravity as opposed to reactions that were conducted under normal gravity (g) and 2–2.5 g (which resulted in larger and poor distribution of gas holes). The authors attributed the uniform and finer porosity of the microgravity synthesized material to be due to non-directional gas release during the reaction, also suggesting their potential application as heat-insulating materials for spacecrafts and space stations. Similar findings with respect to better distributed and finer porosity under microgravity conditions have also been recently reported [49], with the exception of increased amounts of porosity compared to terrestrial gravity, which was attributed to the confining setup used. It should also not be forgotten that highly porous combustion synthesized products can be easily crushed into powders, hence providing for a powder manufacturing process.

Buffering reactions in combustion synthesis

In certain material systems and/or under certain compact pre-heat temperatures, the combustion temperature can equal or exceed the melting point of the product. This can lead to compact shape loss and other defects as mentioned above. To maintain a solid product, the combustion temperature needs to be reduced to below the melting point of the product. This can be achieved for example by using small specimens with large surface area to volume ratio (possibly with the help also of external convective cooling), contacting a small reacting compact with a metal container/punches acting as heat sinks or adding either pre-alloyed (hence already formed) product powder or other composite reinforcements. Here the added powder is considered inert, so it does not add any reactive exothermic component to the rest of the reactive powder mix. Moreover, the added powder particles act as heat sinks to absorb

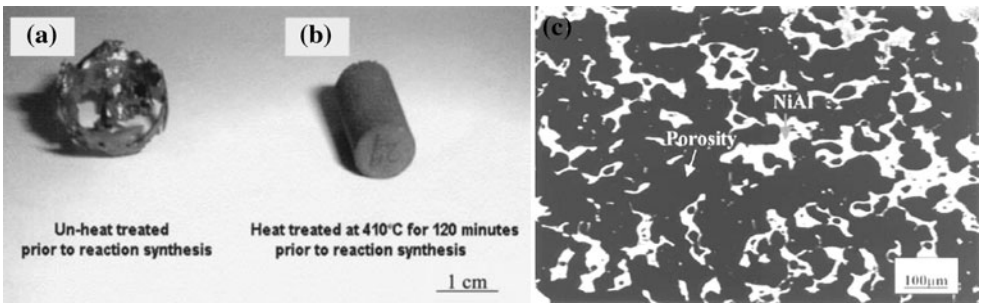

Fig. 3 Effect of Ni + Al green compact prior heat treatment on combustion synthesized (700 °C for 18 min in argon) product. **a** molten NiAl specimen of previously un-heat treated Ni + Al compact, and **b** retained shape of NiAl formed by combustion synthesis of previously heat treated Ni + Al green compact (at 410 °C for 120 min in argon). **c** Porous microstructure of single phase NiAl specimen in (**b**), where all buffering Al_3Ni and Al_3Ni_2 intermetallics have also been consumed in the reaction. [61]

the heat generated from the exothermic reactions emanating from the remainder of the reacting compact. Such an approach has been adopted by many researchers, for example, Alman et al. [128] used 10–25% pre-alloyed NiAl powder in CS studies of Ni–Al to dilute the reaction. Similarly, Morsi et al. [65] used 10% by volume of pre-alloyed Ni_3Al during reactive extrusion work. It should be mentioned though that excessive addition of non-reacting reinforcements can lead to loss of stability in SHS processing and potentially in-homogeneous microstructures. This becomes of particular interest in the manufacturing of composites via CS using inert reinforcements (i.e., not in situ generated composites). For example, for reactively processed intermetallic matrix composites, often mechanically and chemically compatible ceramic reinforcements are added. These have been found not only to reduce the combustion temperature, but also in cases interfere with the process mechanism. For example, in systems where the melting and spreading of a transient lower-melting point phase is an integral part of the CS mechanism, the presence of ceramic (heat absorbing) reinforcements can present obstacles to the pathway of liquid and lead to poor densification and inhomogeneities.

In a recent study by Morsi et al. [66] a different microstructural green compact design was investigated for the CS of Ni_3Al + TiC composites, and compared to conventional green compacts of the same overall reinforcement volume fraction. The design involves embedding the ceramic reinforcements inside the higher melting point nickel powder particles (generating mechanically activated TiC–Ni powder), thus keeping it away from the pathway of molten Al during the reaction. This has led to a substantial reduction in residual porosity from ~25% for conventionally rotator mixed and pressed green compacts to 1.4% for the new microstructural design (without the application of external pressure), also hardness levels were greatly improved.

The interconnectivity of the transient liquid phase during the reaction is very important and is enabled by powder size selection according to percolation theory. For example, the stoichiometric Ni_3Al composition is equivalent to an aluminum volume fraction of 34 vol.%. According to Biggs [54, 67] at such a volume fraction, the aluminum (lower melting point constituent) particle size needs to be at least 2.5 times smaller than that of nickel to achieve percolation/interconnectivity of aluminum particles. Misiolek et al. [54] using agglomerated nickel powder of ~45 μm showed that indeed at aluminum particle sizes greater than 18 μm interconnectivity of the aluminum phase was lost leading to increased product porosity. At increased aluminum particle sizes, in accordance with liquid phase sintering theory, after melting, the capillary force causing densification is also expected to decrease [68], while an excessive increase in volume fraction of the liquid phase can also result in compact slumping. Since the requirement for interconnectivity is indeed important, then it puts practical limitations on the minimum nickel particle size used (since the aluminum particle size needs to be considerably smaller). For example, for nanoparticle reactants this requires the use of nanosized aluminum particles, which have a couple of negative implications. First, at this particle size, nanoaluminum can be pyrophoric and hence dangerous to deal with. Second, at this size a considerable part of the volume of the particle could be occupied by surface oxide, which as mentioned earlier has been shown to cause excessive buffering effects and a reduction in wave velocity [41]. To combat this problem, Morsi et al. [69, 70], embedded/dispersed ultrafine nickel powder in microscale aluminum particles through the process of mechanical milling. This eliminated the requirement for a reduction in aluminum particle size while still maintaining the interconnectivity of aluminum within the Ni/Al particles, which translates to the compact following compaction. The same concept can also be applied to nanosized nickel or other similar reactive systems. In an interesting finding, it has been possible to produce single phase NiAl through thermal explosion (without NiAl melting), by simply growing controlled amounts of aluminum-rich intermetallics (Al_3Ni and

Al_3Ni_2) via solid-state inter-diffusion prior to reaching the ignition temperature. This is carried out through an initial hold at temperatures lower than the ignition temperature, followed by heating to the 700 °C (above the melting point of aluminum). These additionally grown phases helped to control the heat generation of the reaction, provided buffering and prevented the melting of NiAl (Fig. 3), while also being consumed (disappearing) in the reaction resulting in only single-phase solid NiAl.

Activation of combustion synthesis

The inability for certain powder systems to undergo SHS processing has prompted the use of certain effects and processes that enable or enhance SHS behavior/characteristics. As such in this section, mechanical activation through powder ball milling, field activation and microwave activation are discussed as examples.

Mechanical activation

The process of mechanical alloying (MA) of powders has been previously associated with either the dispersion of particles in other particles, to produce unique materials such as oxide dispersion strengthened (ODS) alloys (often referred to as mechanical milling) [71, 72] or more appropriately the "alloying" of the individual particles through mechanical means both of which involve high energy impact of milling balls with the powders. The mechanism of MA (the term used here in its generic form) involves first the deformation of powders under the impact of the balls, followed by work hardening and fracture and eventually their re-welding. For different starting powders this repeated sequence can eventually lead to the atomic mixing of the two or more types of powders to generate alloyed powder. The process boasts a unique advantage over conventional alloying which is an increased or extended solid solubility limit. Due to the impact of the balls with the powder and plastic deformation, the dislocation density and crystallographic defect concentrations within the powders are also increased, which have been reported to give rise to increased high temperature diffusion kinetics through short circuit diffusion [71]. Process variables, include ball-to-powder weight ratio, milling speed, atmosphere, number of milling balls and their size.

When reactive powder mixtures are ball milled, it has been shown that mechanically induced self-propagating reaction (MSR) can occur whereby the powder reactants transfer to products through an SHS type reaction inside the milling vial [73]. If reactive powders are milled up to a time lower than that needed to cause MSR, these powders can remain in the elemental form (as composite particles of the constituent elemental powder) with high reactivity while being refined in terms microstructure (even becoming nanostructured) and can be referred to as mechanically activated [44, 73].

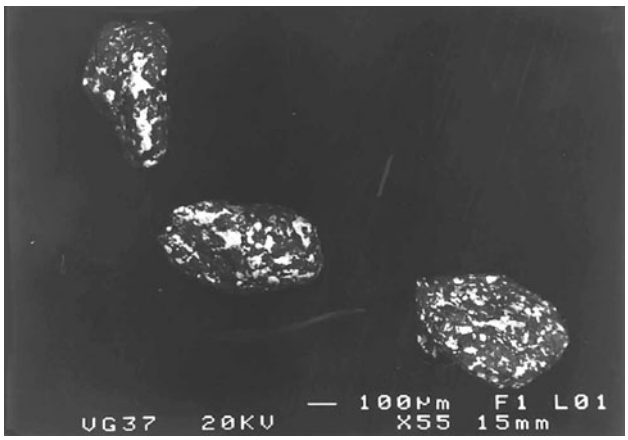

Fig. 4 Mechanically activated "nanostructured" composite powder particles of Nb and Al [76]

The use of such powders in further powder processing such as SHS or annealing, has given rise to the processes of mechanically activated self-propagating high temperature synthesis (MASHS) [74] and mechanically activated annealing process (MA2P) [44], respectively. SHS processing of mechanically activated powders has been reported to produce nanostructured products, increased SHS wave velocities and reduced ignition temperatures. For example, by controlling the ball milling conditions (using a planetary ball mill), Charlot et al. [75] were successful in producing powder aggregates of Fe and Al. This was achieved by limiting the ball milling duration (in air) in such a way as to avoid a reaction between the elemental species. SHS processing of these now highly reactive powders revealed ignition temperatures ~100 °C less than their turbula mixed counterparts. Oxide formation and multiphase microstructures were reported for MASHS materials of powder experiencing a variety of milling conditions. However, conditions were obtained where nanostructured single phase FeAl was produced within the volume of the product (i.e., away from the surface, where Fe_2O_3 and Fe_2Al_5 were also observed on the heated and end faces). Both MASHS and MA2P have been used to produce niobium aluminide, $NbAl_3$ [76], XRD analyses have shown a reduction in the crystal size for both Nb and Al to the nanoscale with an increase in milling time (Fig. 4 shows mechanically activated "nanostructured" composite powder particles of Nb and Al). An interesting finding is that the mode of ball mill operation can in fact influence the subsequent reactive process. For example, the direct shock mode operation of planetary ball mill (G5) was found to be more effective in producing single phase $NbAl_3$ after MA2P of powders for 1 week at 600 °C as compared to the friction

mode. For both direct shock and friction modes, $NbAl_3$ was produced as a major phase using MASHS with a minor amount of Nb_2Al. The temperature-time profile shows a constant temperature region (plateau at ~647–650 °C) corresponding to a melting event (i.e., Al), followed by an increase in temperature leading to the ignition temperature after which an abrupt increase in temperature is observed. Interestingly, increased milling time resulted in a reduction in time of melting (i.e., shortens the plateau region in the temperature–time profile), time following complete melting to the ignition point and a reduction in ignition temperature (by over 200 °C) compared with the turbula mixed counterpart. Here the friction mode of transferring the mechanical energy to the powder particles was more effective in MASHS and reduced the ignition temperature. The work does show that MASHS and MA2P can be affected by how the mechanical energy is transferred during the ball milling process. In another study [74], molybdenum disilicide ($MoSi_2$) was produced using MASHS (carried out in an inert environment). The mechanical milling process here was found to amorphise the silicon and at prolonged milling conditions even form some minor phases of $MoSi_2$ (alpha and beta). SHS wave velocities were found to increase by a factor of 3 compared with the turbula mixed counterpart which was attributed to the very large interfacial area between the elemental species in the case of mechanically activated powders. High yields (95–100%) of nanostructured α-$MoSi_2$ were obtained using MASHS [74]. Although in MASHS nanometric FeAl and $NbAl_3$ products have been produced, the final densities are still a major problem ~80% for FeAl [75] and ~60% for $NbAl_3$ [44], which have been attributed to the expansion of adsorbed gases in the sample. It may appear that such a problem could be reduced through a pre-MASHS degassing step, and/or the application of pressure during synthesis. Indeed an outgassing step was incorporated in the MASHS of $MoSi_2$ by preheating the compact in an argon environment prior to SHS ignition, however, product porosity levels between 42.4 and 52.3% were still reported.

Work on the SHS of mechanically activated Ti and C to form TiC ($Ti_{50}C_{50}$ and $Ti_{70}C_{30}$) has also shown a substantial reduction in ignition temperature (more than 1,000 °C) and an increase in wave velocity with milling time [73] (Fig. 5). Here a SPEX mill was used with a ball-powder-weight ratio of 1.93:1 and milling times investigated were as high as 660 min. It was not however possible to ignite un-milled powders, showing the importance of mechanical activation in the SHS of this powder system.

Recently, MA (using a planetary ball mill, and a 20:1 ball-to-powder weight ratio) of 3Ni + Al powder has also been followed by thermal explosion mode of CS for the processing of nickel aluminides, here a reduction in both the ignition temperature and effective activation energy for thermal explosion (at a heating rate of 4.7 °C/s) were reported with increase in milling time [77] up to 120 s after which they were almost constant with milling time(milling times were investigated up to 3 min). This is a drastic drop compared with the expected ignition temperature of 640 °C. The observation of these MASHS effects at these relatively much shorter milling times maybe a result of the higher BPR as compared to Ti + C among other factors. Ignition temperatures below 200 °C have been reported at milling times of 120 s and higher. In the Ti + C system, activation energy was not found to be affected by milling time for compositions $Ti_{50}C_{50}$ and $Ti_{70}C_{30}$ (calculated at two milling times for each composition) [73]. It was proposed though that at higher milling times, the ignition mechanism changes from the typical liquid–solid reaction to a solid–solid one due to the increased interfacial areas between reactants. In a recent study by Kovalev et al. [78] using time-resolved X-ray diffraction it was found that for mechanically activated Ni–Al mixtures the reaction did not proceed through the formation of an intermediate liquid phase which is typically observed for un-mechanically

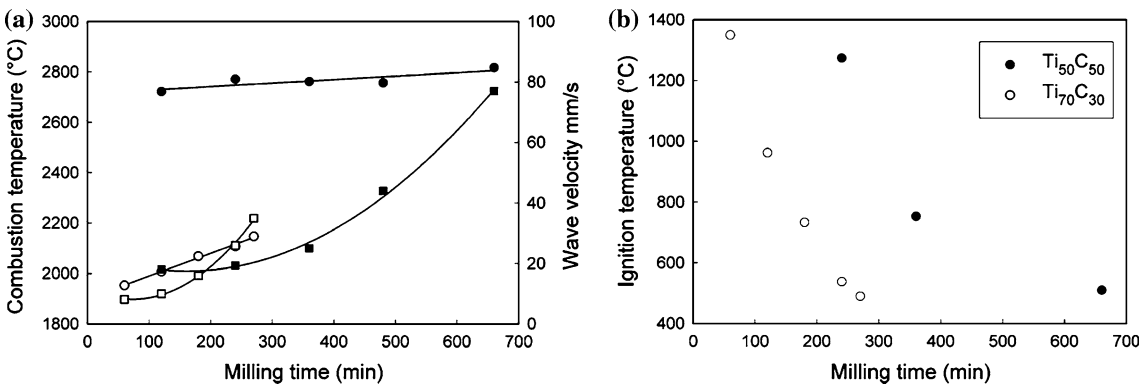

Fig. 5 Effect of milling time on **a** combustion temperature and wave velocity (*square points* are velocity and *circular points* are combustion temperature, *filled points* are $Ti_{50}C_{50}$ and *unfilled* are $Ti_{70}C_{30}$) and **b** ignition temperature for $Ti_{50}C_{50}$ and $Ti_{70}C_{30}$ [73]

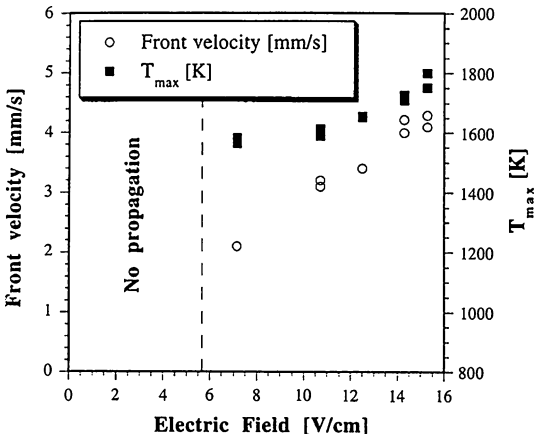

Fig. 6 The effect of applied electric field on the wave velocity and maximum temperature in the synthesis of TiAl [39]

activated powder. Hence traditional reaction mechanisms can be affected/altered by mechanical activation.

Although SHS activation and the reduction of ignition temperatures are possible using MASHS, the presence of substantial residual porosity is still a major problem if high performance structural materials are the objective, which would necessitate the application of pressure. Consequently, mechanical activation and CS have been further combined with spark plasma sintering, extrusion and forging as will be discussed later.

Electric field/current activation

As mentioned earlier for reactive powder systems with low exothermic heats of formation, SHS is not possible at room temperature in the absence of compact preheating. However, as also mentioned, preheating can in fact pose other problems such as pre-combustion phase formation [79]. It has already been shown that mechanical activation is one way to overcome this problem. Another way is through the application of an electric field. For the titanium aluminides it was shown that at some critical value of electric field it was possible to initiate sustained SHS wave propagation [39]. Through a combination of green density and electric field optimization it was shown that low density and high electric field did not only enable SHS reactions but also resulted in the production of single phase Ti_3Al. This was not the case though for TiAl synthesis, where a second phase (Ti_3Al) was also present even at the highest applied field of 15.7 V/cm. The formation of single phase was linked to a second "after burn" peak in the temperature–time profile. In these experiments an in situ monitoring of resistance, voltage and current enabled the elucidation of effects of field and density. Figure 6 shows the effect of applied field on the wave velocity and maximum temperature in the synthesis of TiAl. The figure not only shows a critical field above which SHS is achieved, but also shows an increase in wave velocity and maximum temperature with applied field. In systems such as SiC [79], at very high fields ($\geq$21 V/cm) the reaction mode has even been reported to transition from self-propagating high temperature synthesis to volumetric combustion, requiring no ignition coil source.

Further, in a separate study, for the formation of Ti_3Al, Orru et al. [80] used electric field to both initiate and extinguish (by shutting electric field off) the SHS reaction. A mechanism for phase formation was proposed based on the findings, which involves the initial reaction between molten aluminum and titanium to form Al_3Ti around titanium particles, followed by a gradual increase in Al_3Ti layer and the consumption of aluminum until all aluminum has been depleted. The reaction continues with the reaction between the Ti core and $TiAl_3$ to form Ti_3Al and an outer layer of TiAl. The reaction is then followed by the consumption of Ti core and TiAl layer leading to an increase in Ti_3Al amount until a single phase of Ti_3Al is formed. Despite the production of single phase Ti_3Al, it was clear that porosity levels were also appreciable in the final microstructure. Typically in field-assisted experiments [39], although when field is applied an initial current of 10 A is maintained, during the reaction it was found to rise to much higher values even above 300 A depending on the conditions (the increase in current was accompanied by a reduction in voltage values). Joule heating is hence believed to contribute additional heating to the exothermic heat generated. Whether the product is electrically conductive or not has been shown to have a considerable effect on the wave propagation characteristics. For example, work on silicon carbide synthesis via field-activated SHS has shown a localization of the field effects (Joule heating) only within the narrow combustion zone/layer [79]. Sustained wave propagation is achieved above a critical field level with wave velocity increasing with field strength. At very high field strengths volumetric combustion takes place. Interestingly for electrically conductive products, the localization of current in the reaction zone is lost and for a given field the wave velocity can be found to continuously decreases as the wave propagates along the specimen, an example of this is the field-activated SHS processing of Nb_5Si_3 [81].The decline in wave velocity may even lead the extinction of the wave at some point [79]. The wave velocity and wave temperature can however increase significantly with an increase in the applied field. For example, in the FACS of Ti_3Al, by increasing the field from 6 to 16 V/cm the wave velocity was increased by a factor of 15 while the wave temperature was increased from 1,200 to 1,800 K [39]. In situ measurements during FACS studies can be extremely valuable in elucidating reaction mechanisms, for example, recently Caboura et al. used in situ

time-resolved TRXRD to study current activated SHS sintering of $MoSi_2$ [82].To date, the benefits of the application of field have been well documented in allowing the successful implementation of SHS technology to otherwise non-favorable powder systems. However, its intrinsic influence or use for product densification has not been generally demonstrated in the absence of pressure.

A sister process to field-activated sintering is spark plasma sintering (SPS) which allows the application of both high levels of pulsed electric current (at low voltages) and moderate pressures. It can be regarded as a current-activated hot pressing setup, due to its similarity with hot pressing with the exception that heating is normally provided by direct pulsed electric current through the graphite punches. The process has been used by numerous researchers to sinter powders (metallic, intermetallics, ceramics, and composites) at considerably lower temperatures and times than conventionally possible. The considerably high heating rates have been also seen as a contributing factor to the ability of the process to retain the nanostructure when sintering nanopowders. Recently, Chen et al. [83], studied the SPS of TiAl from ball-milled elemental powders of Ti and Al (Ti–47at.%Al). The sintering temperature was found to considerably influence the densification of the product, but not the multiphase microstructure which consisted of TiAl as a major phase with Ti_3Al and Ti_2Al as minor phases. Despite the formation of nanostructured TiAl at 800 °C, optimum inter-particle bonding and full density were not achieved. SPS at 900 °C provided a good combination of grain sizes <500 nm and near full density product. Interestingly in a separate study by Mei and Miyamoto [84] using elemental powders of Ti and Al of almost similar starting composition (Ti–48%Al), and lower pressure (13 MPa as opposed to 50 MPa), the specimen density following SPS was also seen to increase with temperature, with 1,100 °C and higher yielding comparable densities to Chen et al. The reactively spark plasma sintered Ti and Al mixtures was found to always generate materials with improved densities over the pre-alloyed TiAl powder sintered under the same conditions [84]. However, the predominant phase following SPS was Ti_3Al, but following post-SPS heat treatments TiAl was observed to be the major phase. This may possibly be attributed to mechanical activation, since the elemental powders were ball milled in the first study. An increase in SPS temperature caused excessive TiAl grain growth reaching 500 nm–1.5 μm at 1,100 °C for ball-milled powder which is counterproductive [83]. With the vast majority of SPS work (for reactive as well as non-reactive powder) temperature is usually stated as a predominant processing parameter, when in fact electric current intensity or density should also be mentioned (due to its intrinsic effect). In an interesting study on the reactive processing of Ti and Ni, Locci et al. [85] indeed investigated the effect of AC current density (4,585–5,290 kA/m^2, using a uniaxial pressure of 110 MPa) on the phase formation of Ni + Ti turbula mixed powders. The study shows the effect of electric current intensity, such that only above a critical current intensity (800 A) reaction products were generated. These products were a mixture of phases as opposed to single phase NiTi, but it was shown that the amount of secondary phases decreased with increase in current intensity. This shows a positive effect of current and provides important insight, however in these experiments electric current and temperature were not decoupled (which is not an experimentally trivial matter), such that the higher the currents investigated the higher the temperatures observed due to Joule heating. This leaves the underlying question, what is affecting the process, temperature or current, both of which should have legitimate contributions. If temperature and current are somehow decoupled, it could show the intrinsic effect of current. This has been recently elegantly carried out for non-reacting powders by using a novel setup that allows variation of current while maintaining the temperature constant, showing clear and unequivocal evidence of electric current enhancing solid-state sintering of metallic particles [86]. Although difficult to apply following ignition and especially during the abrupt temperature rise in SHS, it may be interesting to investigate such current effects at temperatures leading up to the ignition temperature, and possibly its effect on wave velocity and ignition/combustion temperatures following local SHS ignition.

Mechanical activation has indeed also been coupled with field/current activation in a number of investigations [87–91], typically much improved densities over MASHS processed materials are obtained in short processing time. In an interesting approach, infrared thermography in conjunction with time-resolved X-ray diffraction were used to capture the thermal and structural evolution of mechanically activated Mo–Si powder under current-activated SHS sintering conditions (excluding the consolidation step). These types of studies greatly help in increasing our understanding of such processes. Preliminary investigations on the localized current-activated CS has been recently conducted by Numula et al. using reactive current-activated tip-based sintering [92]. Electric current was passed through a small (1 mm diameter) tungsten tip which contacts centrally the top surface of a nickel and aluminum green compact, generating a very high current density $\sim$12.7 kA/cm^2. The work resulted in the formation of intermetallics in addition to tungsten contamination (due to reaction with molten aluminum) that traveled to depths below the surface with the aid of molten reactive aluminum. A new approach is currently under investigation that avoids such tip contamination.

Microwave-assisted/activated combustion synthesis (MACS)

The use of microwave energy in conjunction with CS have been reported for a significant number of material systems, composites and coatings [93–100], with some studies making use of domestic microwave ovens to conduct their research. Microwave heating involves heat generation within the compact via material–microwave interactions as opposed to the conventional means of heating which usually travels inwards from the external boundaries of the material. A considerable number of reactive powder systems involve a metallic component. Although bulk metals are known not to couple well with microwaves and would normally reflect them, however due to very small and limited skin-depth microwave absorption levels, metal powders with their small dimensions have been shown to volumetrically heat due to microwave interactions [93, 101]. Ahn and Lee studied the microwave-assisted CS processing of mixtures of silica and aluminum (flake shape, average particle size 23 μm) under a nitrogen environment to produce Sialon [93], utilizing the microwave energy to combine both SHS and nitration in one single step. Powder mixing procedures were found to have a pronounced effect on the ignition characteristics of the mixture. For example, when the powders were mixed using a pestle and mortar for 2 h, it was not possible to ignite the mixture even after 15 min of microwave exposure. However, ball-milled powders using alumina balls were found to ignite, with time-to-ignition considerably decreasing with increase in ball milling time. The authors attributed this to a reduction in particle size with increase in ball milling time as confirmed through SEM analysis. Gedevanishvili et al. [94] have shown that preheating metal powder compacts to a critical temperature can enable enhanced microwave coupling and self-heating through microwave–material interactions. Moreover they have used microwave 'sintering' in conjunction with CS to form a wide range of intermetallics and alloys including binary and ternary compositions, reporting that for most cases ignitions start internally from within the compact. Microwaves can either be switched off immediately following the reaction completion or be kept following the reaction as a form of sintering, here the higher temperature supplied by the CS reaction is effectively used for enhanced microwave absorption. Moreover enhanced microwave–material interactions/absorption with increased input power at the reaction zone during SHS can increase wave velocities and combustion temperatures [93]. An increased combustion temperature has also been reported in the MACS of titanium aluminides from elemental powders, compared with furnace heated compacts (thermally activated combustion synthesis, TACS) [95]. For off-stoichiometric powder mixtures of TiAl and Ti_3Al, MACS allowed the formation of TiAl with minimal Ti_3Al second phase while generating single-phase Ti_3Al, respectively. These results were not matched by TACS or conventional SHS experiments on the same compositions; and porosity was evident in all products. In another study, Blair et al. [99] using metal halides ($AlCl_3$ and $TiCl_3$) precursors with a reducing agent (i.e., Mg) formed pure TiAl via MACS, which was not achieved when the reaction was initiated using a heated filament. The sublimation of $AlCl_3$ has been found to be an important factor that causes an increase in the wave velocity. Thallium superconducting phases, and perovskites were also recently produced via MACS, in addition to coatings such as Ni–Al–Ti [96, 100]. Activity in this area appears to be growing.

Bulk deformation/compaction processes and combustion synthesis

Processes such as hot extrusion, equal channel angular extrusion, hydrostatic extrusion, spark plasma extrusion, SPS, forging, rolling, isostatic pressing, pseudo-isostatic pressing, and uniaxial pressing have all been so far combined/associated with CS processing in many studies. Here we classify the use of bulk deformation/compaction processes in conjunction with CS, in three categories; (1) Bulk deformation/compaction of powder with no or limited reactions between its powder constituents, followed by CS processing as a separate and distinct process or processing cycle. This will be referred to as "Bulk deformation/compaction followed by Combustion Synthesis"; (2) Simultaneous bulk deformation/compaction processes in conjunction with CS within the same process cycle. Again this will be referred to as "Combined Bulk Deformation/Compaction–Combustion Synthesis Processing", and (3) CS of powder compacts followed by the use of bulk deformation of the combustion synthesized product as a separate step for either improving microstructure or further consolidation. The latter category will not be discussed here, since it is regarded as a post-CS processing operation, and does not directly interfere with actual CS mechanisms.

Bulk deformation/compaction followed by combustion synthesis

There have been many studies that use bulk deformation/compaction processes to produce the green compact or body. The simplest of which is pressing, which represented the vast majority of pre-combustion synthesis powder compact preparation methods. However, this too has taken many forms. Due to the microstructural density distributions that can arise when uni-axially pressing powders via single-action die compaction into pellets (this problem is greatly reduced though when pressing thin specimens in

relation to compact diameter, i.e., squat specimens), either double-action die compaction methods or most preferably isostatic pressing [43] have been used. It was recently suggested that due to well known effects of green densities on SHS characteristics, it was advisable to routinely use iso-static pressing in SHS work [33], thus minimizing/eliminating any density distributions within the compact prior to SHS investigations.

Although powder pressing is a universally accepted means for material preparation prior to CS, other methods have also been used. For example, Wang and Dahms [102] used cold extrusion (using two different extrusion ratios [i.e., cross-sectional area reduction] 17:1 and 350:1) to consolidate titanium and aluminum powder mixtures followed by CS at 1,350 °C (for 6 h) in vacuum. Unlike pressing, extrusion involves a significant amount of shear deformation and consolidation which can give rise to highly consolidated green bodies. Even at 17:1 extrusion ratio, less than 0.5% pore content in the green extrudate was reported, becoming zero at 350:1 extrusion ratio. A general feature of the low temperature extrusion of metallic reactant powder is particle elongation in the extrusion direction [42]. This can later have the effect of reducing inter-particle diffusional distances between the different powder reactants. Moreover from an energy prospective, higher extrusion ratios at room temperature have been suggested to increase energy content of the extrudate due to cold working [102] (due to an increase in crystallographic defect concentrations), which may have positive effects on CS. Having a fully dense green body does not however automatically translate to a fully dense product. Again Kirkendall porosity has been reported to occur in systems such as Ni–Al and also Ti–Al where aluminum easily diffuses in titanium (which is not reciprocated by titanium). In an interesting study, Fu et al. [43] examined the effect of powder compacting methods on the CS of Ti–Al. Cold isostatic pressing in addition to hot pressing and extrusion (the latter two were conducted at temperatures between 300 and 400 °C, i.e., below temperatures expected to form interfacial compounds) resulting in consolidated un-reacted elemental powders. The hot extrusion method again gave rise to the highest relative green density (99%).

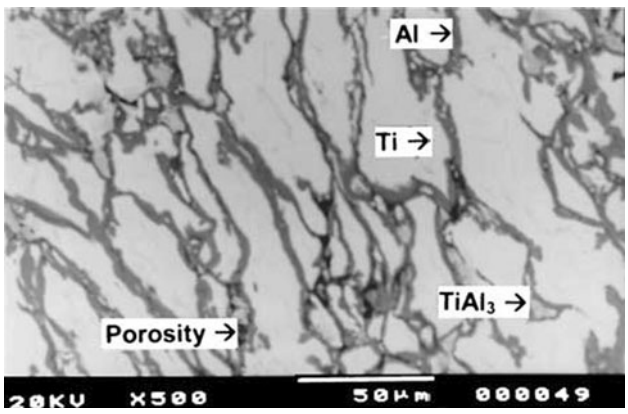

Fig. 7 SEM micrograph showing microstructure of extruded Ti–19 wt% Al after heat treatment at 525 °C for 5 h, showing elongated particles and the formation of $TiAl_3$ [43]

Interestingly, even after prolonged heat treatments (between 500 and 600 °C) up to 36 h, Al_3Ti was the only interfacial product formed between Al and Ti particles through solid-state diffusion (Fig. 7). The compaction of elemental powder is not restricted to conventional pressing or direct extrusion. For example, the production of fully dense Ni + Al powder mixtures in only 1 s at temperatures equal to and lower than 300 °C was recently achieved by the use of ultrasonic powder consolidation [103]. In a recent study by Morsi et al. [104] equal channel angular pressing (ECAP) was also used to consolidate Ti + Al powders (with the view of mechanically activating the powder mixture in bulk form), followed by CS experiments under argon atmosphere. Homogeneous reacted product microstructures were observed only for green bodies that had undergone ECAP for three passes, however no change in ignition and combustion temperatures were observed even up to three passes. It is still possible though that an increased number of passes may promote more pronounced mechanical activation effects.

Powder injection molding technology has been shown to be effective in aligning chopped fibers in a powder matrix [105]. Its application to CS of NiAl composites involves the binder-assisted extrusion (through a tapered die) of matrix elemental powder and chopped fibers. Here extrusion temperature must be above the binder softening temperature, and a follow up binder burnout stage is required before CS processing in combination with Hot Isostatic Pressing. As such fully dense alumina-reinforced NiAl have indeed been formed [106]. The process has the ability to manufacture quite complex green shapes for further processing. Although not considered bulk deformation/compaction process, green body formation/shaping from liquid suspensions have also been recently conducted using tape casting which is subsequently subjected to CS processing, to produce molybdenum disilicide/alumina functionally graded materials [12]. In another interesting approach, surfactant-based self-assembly has also been employed to produce Fe_2O_3 nanotube/aluminum nanoparticles nanoenergetic thermite, where the self-assembly and the nanotube geometry ensures high interfacial area and very good contact between nanoelemental species [107].

Combined bulk deformation/compaction–combustion synthesis processing

In bulk deformation processes, material heating can arise due to work/energy expended in the process. If such heat is

utilized in conjunction with the consolidation features of bulk deformation, then its application to CS may present good possibilities. Recently such an approach has been manifested in the process of Hot Extrusion Reaction Synthesis (HERS). In this process green compacts are uniformly heated either outside or inside the extrusion container to a temperature less than the typical ignition temperature of the powder mixture, followed by extrusion. The heat emanating from the work of extrusion heats the extruding compact to the ignition temperature. Advantages of the process include the use of reactive elemental powder where extrusion pressure and temperature requirements can be moderate. Early work by Tiang and McLean [108] have resulted in the fabrication of materials with only ~5% intermetallics yield. Following this work, mixture of two intermetallics phases (TiAl and Ti_3Al) were produced [109] but accompanied by ~5% porosity. HERS of Ni–Al and their composites was also conducted covering a large array of process conditions [110–114], leading to ~100% conversion of intermetallics under certain conditions. Extrusion temperatures investigated were between 300 and 500 °C.

Although high intermetallic yield was achieved, due to process/reaction kinetics, the reaction generally occurs after the extrudate would have exited the die, thus bypassing the deformation zone where consolidation could have occurred. This hence leaves some residual porosity in the product. A number of observations have been documented, relating to process parameters. It was found for example that when the extrusion temperature (for elemental nickel and aluminum powder) was raised from 350 to 490 °C, instead of a lowering of extrusion pressure (due to an expected decrease in flow stress), a substantial increase in the required extrusion pressure was observed, posing limitations due to extrusion tooling [113], and the material would not extrude as the set load limit was exceeded. The anomalous increase in pressure was attributed to the formation of hard aluminum intermetallics via solid-state interdiffusion. Minay et al. [115] observed a similar event when extrusion of 3Ni + Al powder compacts was attempted at 550 °C, but noticed an unusual and significant dip in the load at a given displacement (when examining the load vs. ram displacement plot). This was attributed to reaction events. Subsequent microstructural characterization revealed that all aluminum was consumed in the reaction, leaving a mixture of phases in the compact (Ni_3Al, NiAl, and Ni). Increasing the extrusion speed was found to result in partial extrusion. Also under certain conditions especially for the more exothermic reactions such as the Ni + Al → NiAl (in the absence of any internal buffering), molten materials would exit the die upon extrusion, presenting safety concerns. To combat this problem a specially designed small-scale extrusion rig was introduced by Morsi et al. [116] that allows not only containment of the extrudate within a bolster, but also allows for visual inspection of the small-scale extrudate as it exits the die, direct temperature measurement and the ability to extrude under atmospheres (e.g., inert).

Recently, Minay et al. [117] reported work on HERS of Ni_3Al, in which the extrusion temperature was increased to 600 °C. By varying the steady-state billet temperature, billet hold time at temperature prior to extrusion (2–12 min) and extrusion speed, it was possible to produce relatively long extrusions. A mixture of phases resulted, with Ni_3Al and Ni as the dominant phases [117]. Witczak et al. [118], encapsulated and evacuated powder compacts of Ni and Al (50/50) in a steel can, heated to 500 °C, then placed in a pressure vessel to apply "hydrostatic extrusion" which resulted in reaction due to the work of extrusion (a 4:1 extrusion ratio was used), there was evidence of product melting in addition to considerable central porosity. Product melting was also observed previously in HERS of NiAl [111], due to the higher exothermic nature of the Ni + Al reaction, thus requiring buffering strategies. In Witczak et al.'s work reacted samples were further hydrostatically extruded at 950 °C to virtually eliminate the porosity and refine the grain structure. Elemental powders have also been canned and either hot extruded or hot forged at elevated temperatures to produce γ-TiAl–Mn–Mo [119].

Work by Kecskes et al. [120] investigated the equal channel angular extrusion (ECAE) of nickel coated aluminum powder for two different compositions Al–22Ni and 23Al–61Ni at temperatures up to 700 °C have resulted in multiphase microstructures, and in some cases cellular. It was found that powder encapsulation in nickel was more effective in terms of consolidation as opposed to copper.

Recently a number of interesting studies were conducted on the reactive forging of interpenetrating phase composites [121, 129] and Ti_3SiC_2 based ceramics [122] producing highly dense final products. In these studies green powder compacts were placed between two heated rams (also used to heat the compact at high heating rates) and a pressure was applied immediately after the onset of thermal explosion. To prevent liquid phase from spreading a confining die was typically used in the setup at the higher applied pressures. In a separate study, the reactive forging setup was also used to estimate the activation energy for thermal explosion of Mg–Si [123].

Mechanically activated elemental powders of equiatomic Ni + Ti were also reactively extruded and forged (Mechanically Activated Reactive Extrusion Synthesis (MARES) and Mechanically activated Reactive Forging Synthesis (MARFOS) respectively) at temperatures at or below 700 °C (with and without elevated temperature (500 °C) degassing sequence in the case of extrusion) in

studies by Neves et al. [124–126]. The products were typically multiphase in nature with remaining un-reacted nickel and titanium in addition to other intermetallics byproducts, thus requiring subsequent heat treatments. The level of porosity was however greatly reduced to a small amount or ~5–9% [124, 125] compared with the high levels typically seen in MASHS work.

A point that has not so far been given a wide adoption is that there does exist a high temperature processing window after the material reaches the combustion temperature and starts to cool, where the material may be malleable and most suitable for shaping (if above the ductile-to-brittle transition temperature [25, 127]) and consolidations. This transient processing window is of short duration, due to heat losses to the surroundings, but is still long enough for rapid processing to occur [20, 33, 130–132]. Hence the "timing" of pressure applications is critical in such reactive bulk deformation work. In systems where a transient liquid phase is present during the reaction, it may not be advisable to apply the pressure during the reaction. For example, in reactive hot isostatic pressing of nickel aluminides, Alman et al. [128] reported in-homogeneities due to non-uniform spreading of the transient liquid due to the application of pressure during the reaction. Recent work on the in situ reactive forging of interpenetrating Al_2O_3/titanium aluminide composites, has shown that the application of pressure during the reaction (while titanium aluminides are in the molten state), can result in the squeezing out of the molten phase leaving high levels of alumina in the center of the compact and mainly titanium aluminide at the peripheries [129]. A confinement cylinder was hence used to avoid such effects. The presence of a transient or otherwise liquid phase during hot extrusion reaction synthesis has also been shown to result in extrudate cracking upon the material exiting the confining extrusion die [111]. Hence it becomes a logical conclusion that an appropriate time to apply pressure could be just after the material reaches the combustion temperature and as it starts to cool down, especially if a liquid phase is not likely to be present. In situations where a single phase product is partially or totally molten, reactive squeeze casting or other forms of casting may be appropriate. Early examples of combining SHS mode of CS with extrusion (SHS extrusion) was carried out by Podlesesov et al. [130], Merzhanov et al [131] and Stolin [132], covering refractory materials such as TiC, TaC, Cr_3C_2, TiB in conjunction with a metallic binder such as nickel, chromium, molybdenum, cobalt or reactive binders such as Ni–Ti to facilitate high temperature deformation. In SHS extrusion, time following SHS ignition has typically been used as a process parameter and divided into a combustion or reaction time (τ_c), material structure formation time (τ_s), and working time (material plasticity loss time) (τ_w) for material deformation [131, 132]. The degree of extrusion completion was measured by the ratio of the mass of extruded material to the charge blank mass [131]. Extrusion conducted too early can still retain powdery material, and too much of a delay before pressure application (i.e., above τ_w) can negatively impact extrusion due to product cooling. LaSalvia et al. [127, 133–135] and Hoke et al. [136] studied the CS (SHS mode)/impact forging of TiC, TiC–Ni based cermets, TiC–Ni–Mo, and TiB_2–SiC. In CS-impact forging specimens are typically placed on a heated anvil and the reaction initiated and a gas driven high-speed forging machine was used to produce forging speeds, e.g., 10–15 m/s. After a certain time delay, the forging stroke was applied. For TiC and TiB_2–SiC densities in excess of 96% were reported, in addition to the need for insulation and furnace cooling to reduce effects of thermal shock-induced cracking was reported for TiC.

Using the thermal explosion mode of ignition, and a setup that allows control of deformation speed, pressure, ram displacement and temperature, Morsi et al. conducted experiments on the reactive extrusion of aluminide intermetallics [65, 137], reactive/combustion forging of FeAl [138] and reactive pressing of Ni_3Al [139] at preselected temperatures, speeds, and ram displacements during the high temperature transient processing window. In the latter, statistical analysis was conducted to arrive at response surfaces for the prediction of residual porosity, grain size and microhardness at a given pressure/temperature combination. Predominantly single phase product was formed which was simultaneously consolidated, by programming the load application system to trigger at a predetermined temperature just after the maximum combustion temperature is achieved and as it cools down. Figure 8, shows the successful processing of reactively/combustion forged FeAl at an onset temperature of 1,000 °C (during material cooling from the combustion temperature). The figure shows how varying the engineering strain (while maintaining the same strain rates, by ram varying speed) affects compact shape change and pore consolidation.

Advantages of such processing include simultaneous shaping of the product and microstructural modification (consolidation and grain refinement through recrystallization). Figure 9 shows the microstructures of a specimen reacted in the extrusion chamber without extrusion and one that has been reacted and extruded as the specimen cools down from the combustion temperature [140]. Grain refinement through recrystallization and consolidation are clear, leading to increased hardness and even superior high temperature oxidation resistance.

Recent work utilizing a setup that involved integrated induction heating capability, investigated the reactive type extrusion of Ni_3Al and Ni_3Al–1B [141]. The approach involved placing the elemental powder in the setup,

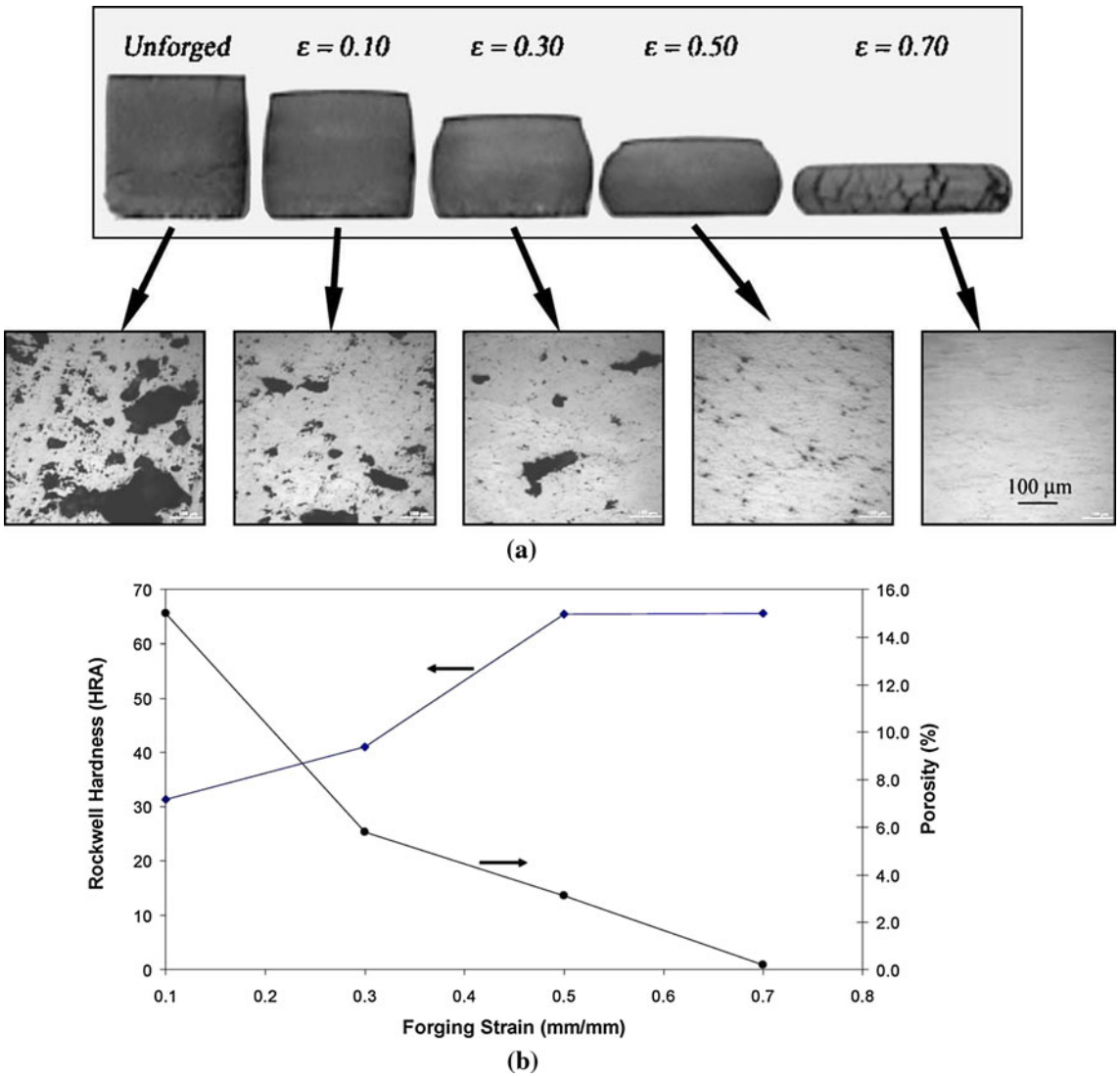

Fig. 8 **a** Combustion synthesized and combustion forged specimens at an onset temperature of 1,000 °C (forging strain (ε) 0.1–0.7) also showing microstructures with corresponding porosity reduction with strain and **b** effect of forging strain on Rockwell hardness and % area porosity. [138]

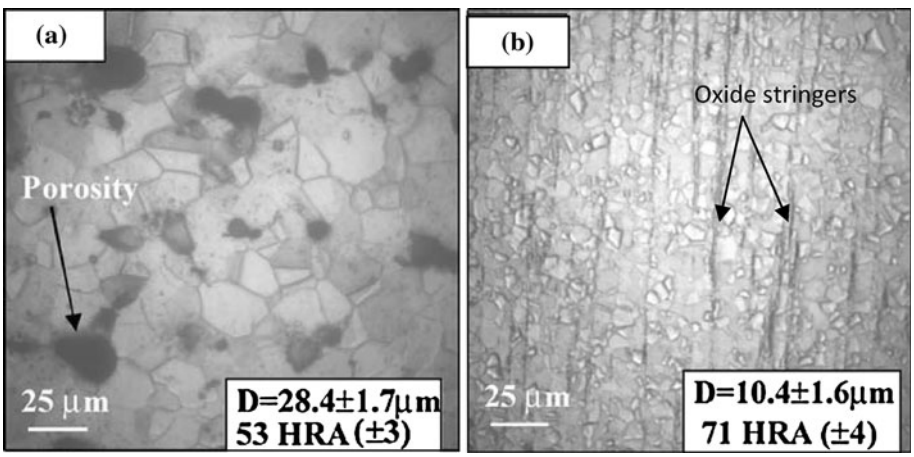

Fig. 9 Micrographs showing microstructures, average grain size (*D*) and Rockwell hardness (HRA) of **a** specimen reacted inside extrusion chamber but not extruded, **b** reacted and extruded (extrusion speed 10 mm/s) at 1,000 °C as the specimen was cooling from the combustion temperature [140]

pressing into compacts and then heating the punch to 480 °C, as soon as a rapid increase in temperature was observed, a delay 2 s was followed by an application of a constant pressure of 400 MPa to allow extrusion. Ni_3Al, Ni and alumina dispersoids were observed in the resulting microstructure, when boron was added NiAl and Ni_3B rich particles where formed in the Ni_3Al–1B alloy.

The present author believes that there are a number of issues that can facilitate the reactive thermomechanical processing of powder. If possible it would be important to obtain direct (full contact) in situ rapid temperature measurements to guide process investigations. For example in recent work on reactive extrusion a thermocouple was typically inserted in the green compact through the die hole [65]. Knowledge of conventional CS processing of material systems should be used effectively to optimize process parameters such as green density, particle size, heating rate, atmosphere and stoichiometry and characterize the high temperature processing window (in terms of duration and reactant-to-product conversion), even prior to reactive thermomechanical process application. Although it still may be possible for the thermomechanical process under certain conditions to improve on and even complete, slightly incomplete reactions. Tool design is also an important issue; for example a conical die in extrusion should promote lower extrusion pressures as opposed to a flat die, since it avoids the need to generate a dead metal zone. However, such a die could also provide for an increased heat transfer to the tooling thus limiting the process. The choice of whether to can the powder or not, is another consideration. Lubrication is yet another important consideration, some lubricants can be chosen for example to also provide a small heat barrier as a dual function. A well-instrumented setup is also required for such investigations, control of pressure, speed (rate) of deformation, displacement and atmosphere, would be a great advantage. Although appears demanding at first, most of these can be accomplished quite easily by designing a setup that can be attached to a fully instrumented universal testing machine [65, 116].

Recently, a spark plasma extrusion approach was reported by Morsi et al.[142], where electric current was used to heat aluminum and aluminum carbon nanotube composites [143, 144] directly to the extrusion temperature, followed by extrusion under current. The approach was preliminarily investigated recently for reactive mixtures of Ti and Al [145], this is the subject of ongoing work by the present author's research group for TiAl and a large number of other reactive mixtures for other systems including mechanically activated ones. For the combination of SHS with rolling, a patent exists to form ceramics [146], vacuum is maintained throughout the process by the evacuation of a can. Combination of SHS with rolling in vacuum was also recently discussed by Chernyshev [147]. This is certainly an area that could benefit from increased levels of research as it has very good potential for mass production.

Alternatively the application of very high pressures (up to 2 GPa) has allowed the fabrication of 98.2% dense single phase NiAl at low temperatures, e.g., 500 °C (hence below the eutectic temperature of 640 °C) through a solid-state reaction [148, 149]. High pressure reaction synthesis of TiB_2/NiAl composites was reported by Bhaumik et al. [150]. Here nickel and aluminum powder were mixed with TiB_2 to composites with 10, 20 and 30 vol.% NiAl. The mixtures were heated to 900 °C under a pressure of 3 GPa, resulting in reaction products consisting of NiAl and Ni_3Al. Further annealing was required to obtain an NiAl matrix. Residual porosity of only $\sim$1% was possible for NiAl vol.% of 15 and higher. However, annealing of such products was found to increase the level of porosity, due to expansion of volatile impurities and adsorbed gaseous species [150]. Recently Dumez et al. [151] also studied the high pressure self-propagating high temperature synthesis (HPSHS) of NiAl intermetallics.

Integral to the SPS process is the application of a uniaxial pressure similar to hot pressing, hence CS–SPS would be appropriate to discuss here. However, the combination of CS with SPS has been discussed in the "Electric field/current activation" section of this article.

Other combustion synthesis-related processes and effects

Reactive casting

The Exo-melt^{TM} process for the reactive melting of iron and nickel aluminides for subsequent casting was demonstrated by Sikka et al. and Deevi et al. [152–154] who used the exothermic energy generated in CS to melt nickel and iron aluminide-based intermetallics for casting. For example, for nickel aluminide alloys, the total amount of nickel is separated into two parts, one containing an Ni/Al ratio equivalent to the NiAl compound and the other is placed below, on top of which the alloying elements were added. Here the very high exothermic heat of the Ni + Al $\rightarrow$ NiAl reaction is used and harnessed to generate an overall temperature over 200 °C higher than the melting point of Ni_3Al. The whole melting process can be finished within minutes, which is then followed by pouring of the melt into a crucible. The process has been shown to result in substantial power reductions (e.g., 47%) when compared to the power requirements associated with the normal melting methods/practices [152]. Figure 10 shows the setup also for iron aluminides.

An example of Exo-melt commercialization is the recent production of 110 large scale rollers of nickel aluminide

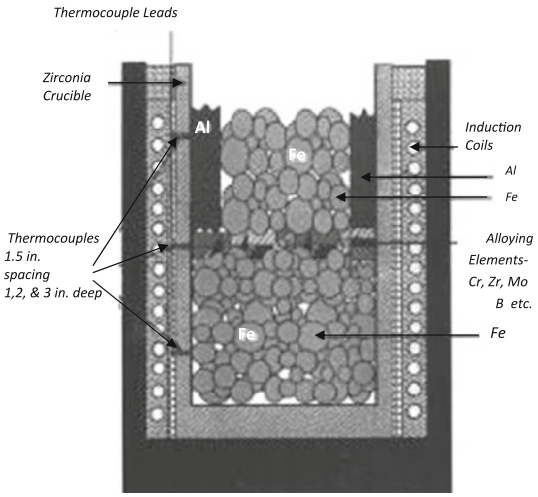

Fig. 10 Schematic of furnace loading configuration in Exo-Melt™ for the melting of iron aluminides [based on 155]

alloy IC-221M for use in steel austenitizing furnaces [156] (Fig. 11).

In another study by Yang et al. [157], using an igniter mixture and low preheat temperature Fe_3Al–$Fe_3AlC_{0.5}$ composites with varying reinforcement loadings were prepared using an SHS casting technique. Inert gas pressure of 5 MPa was applied during the process, and a few pores were only observed in the microstructure. Recently Gorshkov et al. [158] obtained cast molybdenum, niobium, and tungsten silicides via CS under nitrogen atmosphere. Centrifugal casting has also been applied to the field of CS where high gravity (which can reach high levels such as $5{,}000\times g$) is generated that promotes the removal of porosity. A recent example is the melt casting of $Y_3Al_5O_{12}$ (YAG) ceramics (under $900\times g$ acceleration) with the addition of glass to reduce solidification shrinkage cavities and pin grain boundaries thus limiting grain growth [159]. The SHS centrifugal process has also been used to add a ceramic lining to copper pipes [160], and more recently using industrial waste scale and recycled aluminum to produce cermet-lined tubes with superior (more than 20 times) wear resistance compared to uncoated steel pipes [161].

Shock and dynamic (explosive) compaction

The application of explosive compaction type processes to powder mixtures has been adopted by many researchers not only for non-reacting powders but also reacting ones. In the literature there are many names referring to this type of process, these include explosive compaction, shock compaction, shock synthesis, shock-induced reaction synthesis (SRS), and SHS-dynamic compaction. It has been applied to the consolidation of many materials, including ceramics, intermetallics and composites, starting with either elemental or otherwise reacting powder mixtures [162–165]. Typically, the reacting powder is placed in a vessel which is surrounded by explosives that are then detonated [166]. Recently Gur'ev et al. [167] conducted shock wave synthesis of Ti–Al powder mixtures, using a combined dynamic thermal explosion technique with shock compression, and found that the average grain size and shape of the γ-phase was dependent on the high temperature explosive environment condition. In explosive processing (i.e., under extreme conditions), typically, pressure and temperature are rapidly increased due to the shock wave, which can cause extensive amounts of plastic deformation, powder mixing, turbulent flow and powder particle rubbing and fracturing [168]. Reported variations of the process include the use of powder-carrying vessels/capsules of different geometries (i.e., spherical, cylindrical, etc.), shock application to SHS or thermal explosion type reactions, application of pressures through water medium, timing of detonation with respect to pre-reaction, reaction, or post-reaction stage, preheating of the powder reactants. Some experiments include the use of thermocouples to assist in determining the correct timing of detonation while others rely on pre-determined times. Reported advantages of this type of process include the ability to consolidate difficult to consolidate materials such as ceramics and intermetallics, extremely rapid processing (microseconds or less) and cost effectiveness, this is in addition to the ability to apply extremely high pressure levels, e.g., tens of Giga Pascal. In addition to having to deal with dangerous explosives, some of the disadvantages that can materialize in various systems include limited near net shape capability, multiphase product microstructures, generation of microcracks in the product, and also not achieving full densification. Figure 12 shows two typical setups/configurations for combined CS/explosive processes.

Combustion synthesis joining and repair

The use of the exothermic heat generated from the reaction of elemental powders has not only been used to process bulk materials and coatings, but has been applied to the joining of materials. Combustion joining of refractory materials has been recently reviewed by Mukasyan and White [169] covering a number of sub-processes within the volumetric combustion and SHS modes such as reactive joining, reactive resistance welding and combustion foil joining. An example of recent work by Kimata et al. [170] for the joining of spheroidal graphite cast iron with copper alloy (BC6) via a reacting mixture of Ni, Al, and Si. Here an induction heated hot press setup was used under vacuum, to allow heating to 700 °C. Good interfacial bonding on either side of the reacting mixture was reported.

Fig. 11 Different stages in the manufacturing of large scale nickel aluminide rolls for steel austentizing furnaces: **a** cast bodies, **b** machined ends ready for welding, **c** welded trunnion to roll body, **d** weld close-up, **e** enlarged image of weld, **f** rolls, **g** rolls in process of shipping, and **h** rolls prepared for installation [156]

However when Al_3Ni phase was formed in the filler (by varying the initial reactant powder composition) cracking was observed. In another study by Pascal et al. [171], Ni + Al reacting mixtures had a dual use of also generating heat to an already exothermic coating mixture (Ni + Cr + Al + Y) (i.e., similar concept as a chemical oven). Here simultaneous formation and joining of NiCrAlY layer to a Rene 77 super alloy substrate was carried out under an argon hydrostatic pressure of 50 MPa. CS has also been investigated for the repair of gas turbine components, through an SHS build-up process, with advantages that include minimal energy requirements and local treatment that is not spread to the remainder of the component [172]. In a recent study Sytschev et al. [173] investigated the joining of Ni–Al-based mixture to molybdenum foil using SHS.

Laser-assisted combustion synthesis

The use of selective laser sintering (SLS) for rapid prototyping has been around for some time. It is a form of layered manufacturing where 3D objects can be manufactured layer by layer with the use of computer aided design (CAD) model, and the heating effects of a scanned laser spot. Major process variables are laser power and laser scan speed. It has been reported that the SLS of metals is much more challenging and complex than that of polymer systems [174], and atmosphere control is crucial to diminish effects of oxidation (which can result in poor wetting leading to poor layer interfacial bonding), hence, as reported, high vacuum or ultra-high purity inert dynamic atmospheres are usually recommended. Moreover, a process involving partial re-melting of the previously formed

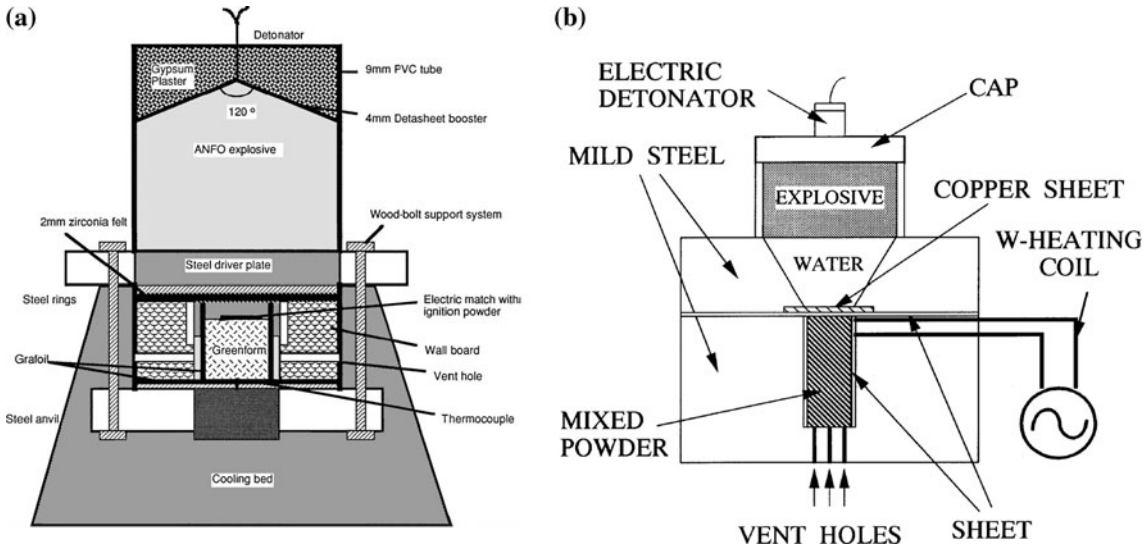

Fig. 12 Schematic diagrams of reactive shock synthesis apparatus **a** without employing water as a medium [163], **b** with water as a medium [165]

layer, and epitaxial heterogeneous nucleation has been identified as the main mechanism for product formation and production of full density products. The use of lasers in the context of CS, can take two forms. The first involves using lasers as a means to ignite the SHS reaction of a reactive powder mix. For example, Li et al. [175] investigated the effect of laser power on the ignition and combustion temperature of Al–C–Ti powder mixtures to form Al/TiC composites. They reported that a reduction in laser power corresponded to a reduction in the combustion temperature. The second form of using lasers comes in their use as an integral part of the processing and not just as an ignition method; here SLS technology plays a combined role with SHS. As such, the combination of SLS processing with SHS has been applied to a number of material systems, including aluminides, titanium nickelide, ferroelectric as well as piezoelectric materials [176], moreover Ni/Ti-hydroxyappatite (HA) composites and porous magnetic complex oxides have also been formed [177], in addition to their combination to form coatings [178]. Figure 13 shows

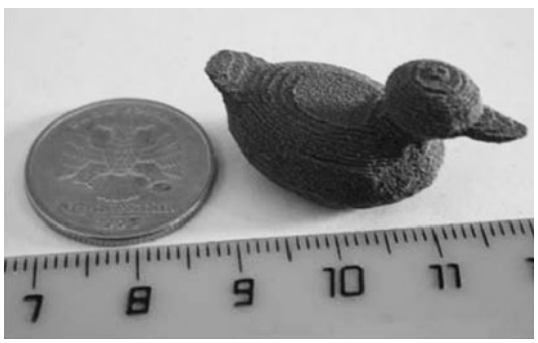

Fig. 13 Small-scale duck shape produced by SLS–SHS [176]

the ability of the process to manufacture relatively complex shapes. The application of SLS to reactive Ni–Ti powder systems was investigated by Gureev et al. [179] where they found that atmosphere played a significant role in whether a controlled (localized) reaction occurred or not. Laser power ranging from 0.5 to 16 W and laser spot diameters of 50 and 100 μm were investigate. Laser-material interactions conducted in air were not successfully localized due to oxidation and subsequent reaction spreading (in a separate study HA was also found to dissociate when processed in an air environment, as opposed to under argon atmosphere [177]). On the contrary, experiments conducted under argon atmosphere generated a controlled reaction zone, which is critical for the successful subsequent building of 3D structures. The 3D structure was porous, and NiTi was identified as a major phase. Synchronizing SHS effects with laser spot velocity is not trivial, this has been modeled in 2D by Zakiev et al. [176] for single layer systems which allows control of such reactions.

Laser sintering conditions have also been successfully selected to obtain conditions where SHS and SLS are in "dynamic equilibrium" [180] allowing the 3D layered manufacturing of metal-polymer, intermetallic and ceramic materials. In a recent study by Shishkovsky et al. [177], SLS/SHS processing of a series of material systems including nickel aluminides, Ni + Ti/HA and functionally graded materials were fabricated. An important identified prerequisite for the successful localization of such reactions to the focused laser beam spot was initially choosing powder system with low predicted adiabatic temperatures (i.e., ones that would not normally undergo SHS type reactions and hence avoid any runaway events). Optimization of the energy density of the laser beam is also

important. Within a controlled workable range, an increase in energy density has been shown to increase the depth of reaction beneath the surface. This is important to make sure reactions totally penetrate through each of the deposited powder layers, and not partially. Energy densities above these workable ranges tend to give rise to a reaction spreading to the remainder of the sample volume, and energy densities below the workable ranges give rise to incomplete reactions [177].

To date good advances have been made in combined SLS/SHS processing, where SLS process parameters (including beam scan speed, energy density and atmosphere) and SHS material selection strategies (i.e., using systems with low adiabatic temperatures) have been effectively utilized to enable the production of 3D artifacts of relatively complex geometries. For more exothermic reactions, in situ temperature measurements that can provide feedback control loop to guide laser processing parameters has been discussed, and evidence of the formation of highly refined intermetallic microstructural features at high laser power inputs have been reported [180]. Moreover in a separate study, it was reported that depending on the material system honecomb, dendritic, or mosaic geometric features were produced [181], and the fractal dimensions were influenced in different ways by laser input energy but had a dependence on roughness. Hence there exists opportunities within this type of processing scheme for the production of new microstructures and potentially unique properties. The process has however so far been largely limited to the production of porous materials, and in cases incomplete reactions at some spots for certain materials. Possibly multiple laser scans per deposited layer may potentially improve on these. Moreover, research into the precise laser/material (reactive powder) interactions may help elucidate the governing mechanisms in operation and together with powder design may provide for a platform for the routine production of pore-free SLS/SHS processed materials in future.

Reactive infiltration

This is an area that has seen a large amount of research activity judging from published work. Its basic principle is first the production of a porous powder-based or pre-sintered pre-form followed by introducing the lower melting point reacting phase/element in the form of a liquid and enable its infiltration through the pores of the perform and at the same time reacting with the preform to produce the intended material. The process gives rise to exothermic product formation and reducing/eliminating initial preform pore content. The process has a number of fundamental variables, which include the superheat temperature of the molten phase, molten phase composition, preform pre-heat temperature, applied pressure and type (i.e., atmospheric, uniaxial, isostatic), pre-form pore size, and pore content. Logically porosity in the preform needs to be open, i.e., interconnected; hence high sintered preform densities containing closed pores would not be suitable. A number of issues have been documented for such processing. First, competition can exist between the rate of infiltration of molten phase into the preform and rate of reaction between the molten phase and preform. If the latter is faster than the former, then typically a process called choking occurs were pores can be blocked by product phases, and thus infiltration is greatly hampered. Pressure can be used to control the rate of infiltration, and unlike typical SHS products, pore free materials have been produced using this technique. Reported advantages [182–184] include avoiding to deal with oxides often present on powder surfaces such as for aluminum powder when molten aluminum is the infiltrating melt. For composites, the integrity of reinforcements such as whiskers or fibers can be protected as opposed to using compaction processes, near net shaping (with the help of molds/crucibles) and rapid processing. Initial preform pore content can play a role in the final product composition. For example, Suganuma [184] showed the final composition changes from Ni_3Al to NiAl and minor phase Ni_3Al when the Ni preform density was changed from 66 to 46% after aluminum infiltration. Moreover, as reported, due to solubility, an infiltrating liquid may dissolve and acquire atoms from the preform as it infiltrates the compact resulting in a final product with compositional variation. Examples of recent work on reactive infiltration include inkjet printing of green bodies followed by binder burnout and infiltration with aluminum [185], production of superconducting MgB_2 tubular wires by magnesium reactive infiltration [186], processing of C/C–SiC dual matrix composites through reactive infiltration of silicon [187], molten silicon infiltration into meso-carbon microbeads-based carbon preform [188], production of nitride ceramic composites through infiltration of titanium nitride with molten aluminum [189], and the production of $NbAl_3/Al_2O_3$ composites through pressure-less reactive infiltration by controlling the perform channel pore size [190]. The activity in this area is high.

Summary

Research activities in the area of CS are constantly growing and diversifying to generate new first, second and multi-level CS-related hybrid processes. Some of these processes/effects have provided means to activate the CS process, improve on reaction characteristics, modify microstructure and phase evolution, and reduce/eliminate the problem of residual porosity.

Processes and effects such as gravity (high and low), mechanical activation, field/current activation, microwave energy interactions, laser–SHS interactions, reactive infiltration, reactive explosive compaction, reactive casting, reactive joining, reactive thermomechanical processing, pre-reaction heat treatment, new green compact microstructural designs are numerous examples from an array of possibilities that have already been investigated in the CS field. However, for some processes and material systems full conversion from reactants to products through CS, and the generation of pore-free products still remain a challenge. It is also apparent that more consideration could be given to the timing of pressure application during reactive thermo-mechanical processing. With prior optimization of reaction parameters, the timing of pressure application during the cooling stage following the reaction could provide benefits for consolidation, complete reaction/phase yield, microstructural refinement (through recrystallization) and product shaping all at once. Moreover, new multilevel hybridization may provide means for combining complimentary benefits of existing processes to produce optimized products. With the current strong activity within the area of CS, the future still holds great promise and opportunities for innovations.

Acknowledgements The author wishes to thank the National Science Foundation (CMMI Division, Materials Processing and Manufacturing program, Grant number 0826532) for their partial support.

References

1. Booth F (1953) Trans Farad Soc 49:272
2. Munir Z (1988) Ceram Bull 67(2):342
3. Merzhanov AG, Borovinskaya IP (2008) Int J Self-Prop High-Temp Syn 17(4):242
4. Holt JB, Munir ZA (1986) J Mater Sci 21(1):251. doi:10.1007/BF01144729
5. Philpot KA, Munir ZA, Holt JB (1987) J Mater Sci 22(1):159. doi:10.1007/BF01160566
6. Munir ZA, Holt JB (1987) J Mater Sci 22(2):710. doi:10.1007/BF01160792
7. Deevi SC (1991) J Mater Sci 26(12):3343. doi:10.1007/BF01124683
8. Zhang S, Munir ZA (1991) J Mater Sci 26(13):3685. doi:10.1007/BF00557164
9. Jeng YL, Lavernia EJ (1994) J Mater Sci 29(10):2557. doi:10.1007/BF00356804
10. Saidi A, Chrysanthou A, Wood JV et al (1994) J Mater Sci 29(19):4993. doi:10.1007/BF01151089
11. Fan QC, Chai HF, Jin ZH (1999) J Mater Sci 34(1):115. doi:10.1023/A:1004430028260
12. Dumont A-L, Bonnet J-P, Chartier T, Ferreira JMF (2001) J Eur Ceram Soc 21(13):2353
13. Groven LJ, Puszynski JA (2008) In: AIChE annual meeting, conference proceedings, November 16, 2008–November 21. American Institute of Chemical Engineers
14. Augustin CO, Selvan RK (2003) Bull Electrochem 19(7):319
15. Xanthopoulou G, Vekinis G (2001) Adv Env Res 5:117
16. Subrahmanyam J, Vijayakumar M (1992) J Mater Sci 27:6249. doi:10.1007/BF00576271
17. Yi HC, Moore JJ (1990) J Mater Sci 25:1159. doi:10.1007/BF00585421
18. Munir Z (1992) Metall Trans A 23:7
19. Dunand DC (1995) Mater Manuf Process 10(3):373
20. Mukasyan AS, Rogachev AS (2008) Prog Energy Combust Sci 34:377
21. Reddy BSB, Das K, Das S (2007) J Mater Sci 42:9366. doi:10.1007/s10853-007-1827-z
22. Mossino P (2004) Ceram Int 30:311
23. Moore JJ, Feng HJ (1995) Prog Mater Sci 39:243
24. Moore JJ, Feng HJ (1995) Prog Mater Sci 39:275
25. Bowen CR, Derby B (1997) Br Ceram Trans 96(1):25
26. Varma A, Rogachev AS, Mukasyan AS, Hwang S (1998) Adv Chem Eng 24:79
27. Varma A, Mukasyan AS (1998) Powder Met Technol Appl 7:523
28. Rogachev AS, Mukasyan AS (2010) Combust Explos Shock Waves 46(3):243
29. Eakins DE, Thadhani NN (2009) Int Mater Rev 54(4):181
30. Vallauri D, At′ıas Adri′an IC, Chrysanthou A (2008) J Eur Ceram Soc 28:1697
31. Cincotti AA, Licheri R, Locci AM, Orru R, Cao G (2003) J Chem Technol Biotech 78:122
32. Grigorieva TF, Barinova AP, Lyakhov NZ (2003) J Nanopart Res 5:439
33. Morsi K (2001) Mater Sci Eng A 299(1–2):1
34. Barzykin VV (1992) Pure Appl Chem 64(7):909
35. Novikov NP, Borovinskaya IP, Merzhanov AG (1975) In: Merzhanov AG (ed) Combustion processes in chemical technology and metallurgy. p 174
36. Munir ZA, Anselmi-Tamburini U (1989) Mater Sci Rep 3(7–8):277
37. Yeh CL, Sung WY (2004) J Alloys Compd 384(1–2):181
38. Bernard F, Souha H, Gaffet E (2000) Mater Sci Eng A 284(1):301
39. Orru R, Cao G, Munir ZA (1999) Met Mater Trans A 30A:1101
40. Sohn HY, Wang X (1996) J Mater Sci 31:3281. doi:10.1007/BF00354680
41. Hunt EM, Plantier KB, Pantoya ML (2004) Acta Mater 52:3183
42. Lee TW, Lee CH (1998) J Mater Sci Lett 17:1367
43. Fu EK, Rawlings RD, McShane HB (2001) J Mater Sci 36:5537. doi:10.1023/A:1012540927009
44. Gauthier V, Josse C C, Bernard F, Gaffet E, Larpin JP (1999) Mater Sci Eng A265:117
45. Locci AM, Licheri R, Orru R, Cincotti A, Cao G, De Wilde J, Lemoisson F, Froyen L, Beloki IA, Sytschev AE, Rogachev AS, Jarvis DJ (2006) ALCHE J 52(11):3744
46. Merzhanov AG (2002) Adv Space Res 29(4):481
47. Odawara O (1997) Ceram Int 3:273
48. Sytschev AE, Merzhanov AG (2009) Int J Self-Prop High-Temp Syn 18(3):200
49. Zanotti C, Giuliani P, Maglia F (2006) Intermetallics 14:213
50. Kirdyashkin AI, Maksimov Yu M, Kitler VD, Lepakova OK, Burkin VV, Sinyaev SV (1999) Combust Explos Shock Waves 35(3):271
51. Filimonov IA, Kidin NI (2005) Combust Explos Shock Waves 41(6):639
52. Munir Z (1992) Met Trans A 23A:7
53. Sims DM, Bose A, German RM (1987) In: Freeby CL, Hjort H (ed) Annual powder metallurgy conference proceedings, p 575
54. Misiolek W, German RM (1991) Mater Sci Eng 144:1
55. Song I-H, Kim D-W, Yun J-Y, Kim H-D (2005) Key Eng Mater 287:226
56. Il'In EN (2010) Refract Indu Ceram 51(1):12

57. Hunt EM, Pantoya ML, Jouet RJ (2006) Intermetallics 14:620
58. Wu-Laitao Luo Y, Liu W (2007) J Chem Sci 119(3):237
59. Kim JS, Kang JH, Kang SB, Yoon KS, Kwon YS (2004) Adv Eng Mater 6(6):403
60. Kobashi M, Inoguchi N, Kanetake N (2010) Intermetallics 18:1039
61. Morsi K, Fujii T, McShane H, McLean M (1999) Scripta Mater 40(3):359
62. Dong HX, He YH, Zou J, Xu NP, Huang BY, Liu CT (2010) J Alloys Compd 492:219
63. Dong HX, He YH, Jiang Y, Wu L, Zou J, Xu NP, Huang BY, Liu CT (2011) Mater Sci Eng A 28:4849
64. Guojian J, Qingxue Z, Hanrui Z, Wenlan L, Maozi L (2001) Mater Res Bull 36:617
65. Morsi K, Moussa SO, Wall JJ (2005) J Mater Sci 40:1027. doi: 10.1007/s10853-005-6526-z
66. Morsi K, Wang N (2008) J Alloys Compd 452(2):367
67. Biggs DM, Bhattacharya SK (1986) In: Metal-filled polymers. Dekker, New York, p 165
68. German RM (1985) In: Liquid phase sintering. Plenum, Troy, New York, p 54
69. Morsi K, Shinde S, Olevsky EA (2006) J Mater Sci 41(17):5699. doi:10.1007/s10853-006-0068-x
70. Morsi K, Shinde S, Olevsky EA (2006) Mater Sci Eng A 426(1–2):283
71. Benjamin JS (1970) Sci Am 234(5):40
72. Suryanarayana C (2004) Mechanical Alloying and Milling. Marcel Dekker, New York
73. Maglia F, Anselmi-Tamburini U, Deidda C, Delogu F, Cocco G, Munir Z (2004) J Mater Sci 39:5227. doi: 10.1023/B:JMSC.0000039215.28545.2f
74. Gras Ch, Vrel D, Gaffet E, Bernard F (2001) J Alloys Compd 314:240
75. Charlot F, Gaffet E, Zeghmati B, Bernard F, Niepce JC (1999) Mater Sci Eng A262:279
76. Gauthier V, Josse C, Bernard F, Gaffet E, Larpin JP (1999) Mater Sci Eng A 265(1):117
77. Korchagin MA, Yu V, Filimonov, Smirnov EV, Lyakhov NZ (2010) Combust Explos Shock Waves 46(1):41
78. Kovalev DYu, Kochetov NA, Ponomarev VI, Mukasyan AS (2010) Int J Self-Prop High-Temp Syn 19(2):120
79. Munir ZA (1997) Solid State Ionics 101–103:991
80. Orru R, Cao G, Munir ZA (1999) Ch Eng Sci 54:3349
81. Feng A, Munir ZA (1997) J Am Ceram Soc 80(5):1222
82. Cabouro C, Chevalier S, Gaffet E, Vrel D, Boudet N, Bernard F (2007) Act Mater 55:6051
83. Chen YY, Yu HB, Zhang DL, Chai LH (2009) Mater Sci Eng A A525:166
84. Mei B, Miyamoto Y (2001) Met Mater Trans A 32A:843
85. Locci AM, Orrù R, Cao G, Munir ZA (2003) Intermet 11:555
86. Frei JM, Anselmi-Tamburini U, Munir ZA (2007) J Appl Phys 101:114914
87. Tsuchida T, Yamamoto S (2004) Solid State Ionics 172:215
88. Paris S, Gaffet E, Bernard F, Munir ZA (2004) Scripta Mater 50:691
89. Heian EM, Khalsa SK, Lee JW, Munir ZA (2004) J Am Ceram Soc 87(5):779
90. El Kedim O, Paris S, Phihini C, Bernard F, Gaffet E, Munir ZA (2004) Mater Sci Eng A369:49
91. Cabouro G, Chevalier S, Gaffet E, Vrel D, Boudet N, Bernard F (2007) Acta Mater 55:6051
92. Numula A, Morsi K, Moon KS, Kassegne SK (2011) In: Proceedings of the 2011 TMS annual meeting, EPD congress. San Diego, CA, p 819
93. Ahn ZS, Lee HB (1998) J Mater Sci 33:4255. doi: 10.1023/A:1004490227256
94. Gedevanishvili S, Agrawal D, Roy R (1999) J Mater Sci Lett 18:665
95. Jokisaari JR, Bhaduri S, Bhaduri SB (2005) Mater Sci Eng A 394:385
96. Boromei I, Casagrande A, Tarterini F, Poli G, Veronesi P, Rosa R (2010) Surf Coat Technol 204:1793
97. Atong D, Clark DE (2004) Ceram Inter 30:1909
98. Golkar G, Zebarjad SM, Khaki JV (2010) J Alloys Compd 504:566
99. Blair RG, Gillan EG, Nguyen NKB (2003) Chem Mater 15:3286
100. Bayya SS, Snyder RL (1994) Phys C Supercond 225(1–2):83
101. Lorenson CP, Ball MD, Shaw H, Herzig R (1990) Res Soc Proc 189:279
102. Wang G-X, Dahms M (1992) Scr Metall Mater 26:1469
103. Erdeniz D, Ando T (2011) In: Proceedings of the 2011 TMS annual meeting, symposium on processing and properties of powder based materials, p 553
104. Morsi K, Goyal S (2007) J Alloys Compd 429:L1
105. German RM, Bose A (1989) Mater Sci Eng A107:107
106. Stoloff NS, Alman DE (1991) Mater Sci Eng A144:51
107. Cheng JL, Hng HH, Ng HY, Soon PC, Lee YW (2010) J Phys Chem Sol 71(2):90
108. Cheng T, McLean M (1996) Mater Let 29:91
109. Cheng T, McLean M (1997) J Mater Sci 32:6255. doi: 10.1023/A:1018689111498
110. Morsi K, McShane H, McLean M (1997) Scripta Mater 37(11):1839
111. Morsi K, McShane HB, McLean M (2000) Mater Sci Eng A 290(1):39
112. Morsi K, McShane H, McLean M (2000) J Mater Sci Lett 19(4):331. doi:10.1023/A:1006770916085
113. Morsi K, McShane H, McLean M (1998) J Mater Sci Lett 17(19):1621
114. Morsi K, McShane HB, McLean M (2000) Metall Mater Trans A 31(6):1663
115. Minay EJ, Sutthispripok W, Rawlings RD, McShane HB (2001) J Mater Sci Lett 20:1979
116. Morsi K, Nanayakkara N, Mcshane HB, Mclean M (1999) J Mater Sci 34(12):2801. doi:10.1023/A:1004666830950
117. Minay EJ, McShane HB, Rawlings RD (2004) Intermetall 12(1):75
118. Witczak Z, Witczak P, Jemielniak R, Mazur A (2004) J Mater Sci 39:551. doi:10.1023/B:JMSC.0000039276.20274.8b
119. Lee TK, Kim JH, Hwang SK (1997) Met Mater Trans A 28:2723
120. Kecskes LJ, Gardiner DM, Woodman RH, Barber RE, Hartwig KT (2006) Met Mater Trans 37:449
121. Horvitz D, Gotman I (2002) Acta Mater 50:1961
122. Khoptiar Y, Gotman I (2003) J Eur Ceram Soc 23:47
123. Horvitz D, Klinger L, Gotman I (2004) Scripta Mater 50:631
124. Neves N, Martins I, Correia JB, Oliveira M, Gaffet E (2008) Mater Sci Eng A 473:336
125. Neves N, Martins I, Correia JB, Oliveira M, Gaffet E (2007) Intermetallics 15:1623
126. Neves N, Martins I, Correia JB, Oliveira M, Gaffet E (2008) Intermetallics 18:889
127. LaSalvia JC, Kim DK, Meyers MA (1996) Mater Sci Eng A 206(1):71
128. Alman D, Stoloff NS (1991) Int J Powder Metall 27(1):29
129. Horvitz D, Gotman I, Gutmanas EY, Claussen N (2002) J Eur Ceram Soc 22:947
130. Podlesesov VV, Radugin AV, Stolin AM, Merzhanov AG (1992) J Eng Thermophys (translated from Russian Journal Inzhenero-Fizicheskii Zhurnal) 63(5):1065
131. Merzhanov AG, Stolin AM, Podlesesov VV (1997) J Eur Ceram Soc 17:447
132. Stolin AM (1992) Int J Self-Propag High Temp Synth 1(1):135

133. LaSalvia JC, Meyers MA, Kim DK (1994) J Mater Synth Process 2(4):255
134. LaSalvia JC, Meyer LM, Meyers MA (1992) J Am Ceram Soc 75(3):592
135. LaSalvia JC, Kim DK, Meyers MA (1996) Mater Sci Eng A 206:71
136. Hoke DA, Do KK, LaSalvia JC, Meyers MA (1996) J Am Ceram Soc 79(1):177
137. Morsi K, Wall J, Rodriguez J, Moussa SO (2003) J Mater Eng Perform 12(2):147
138. Morsi K K, Rodriguez J (2004) J Mater Sci 39:4849. doi: 10.1023/B:JMSC.0000035324.33204.cc
139. Moussa SO, Morsi K (2007) Mater Sci Eng A 454–455:641
140. Morsi K, Moussa SO, Wall J (2006) J Mater Sci 41:1265. doi: 10.1007/s10853-005-4233-4
141. Guo JT, Sheng LY, Xie Y, Zhang ZX, Ovcharenko VE, Ye HQ (2011) Intermetallics 19:137
142. Morsi K, El-Desouky A, Johnson B, Mar A, Lanka S (2009) Scripta Mater 61(4):395
143. Morsi K, Esawi AMK, Lanka S, Sayed A, Taher M (2010) Compos A 41(2):322
144. Morsi K, Esawi AMK, Borah P, Lanka S, Sayed A, Taher M (2010) Mater Sci Eng A 527(21–22):5686
145. Mehra P, Morsi K (2011) Proceedings of the 2011 TMS annual meeting, EPD congress. San Diego, CA, p 803
146. Rice RW (1987) Hot rolling of ceramics by the use of self propagating synthesis. US Patent 4,642,218, 10 Feb 1987
147. Chernyshev VN (2007) Refract Ind Ceram 48(5):359
148. Cheng T, Sun J (1994) Scipta Metall Mater 30:247
149. Cheng T (1996) J Mater Sci 31:1997. doi:10.1007/BF00356619
150. Bhaumik SK, Divakar C, Rangaraj L, Singh AK (1998) Mater Sci Eng A257(2):341
151. Dumez M, Marin-Ayral R, Tedenac J (1998) J Alloys Compd 268(1–2):141
152. Deevi SC, Sikka VK (1997) Intermetallics 5:17
153. Sikka VK, Deevi SC, Vought JD (1995) Adv Mater Process 147(6):29
154. Orth JE, Sikka VK (1995) Adv Mater Process 148(5):33
155. Sikka VK, Wilkening D, Liebetrau J, Mackey B (1998) Mater Sci Eng A 258(1–2):229
156. Sikka VK, Santella ML, Angelini P, Mengel J, Petrusha R, Martocci AP, Pankiw RI (2004) Intermetallics 12(7–9):837
157. Yang J, La P, Liu W, Hao Y (2004) Mater Sci Eng A 382(1–2):8
158. Gorshkov VA, Yukhvid VI, Miloserdov PA, Sachkova NV, Kovalev DYu (2011) Int J Self-Prop High-Temp Syn 20(2):100
159. Liu G, Li J, Guo S, Ning X, Chen Y (2011) J Alloys Compd 509:1213
160. Du Z, Fu H, Fu H, Xiao Q (2005) Mater Lett 59(14–15):1853
161. Andreev DE, Sanin VN, Sachkova NV, Yukhvid VI (2011) Int J Self-Prop High-Temp Syn 20(1):27
162. Sawaoka AB, Akashi T (1987) US Patent 4, p 830
163. Song I, Wang L, Wixom M (2000) J Mater Sci 35:2611. doi: 10.1023/A:1004731532616
164. Thadhani NN (1990) In: Schmidt SC, Johnson JN, Davison LW (eds) Shock compression of condensed matter. Elsevier, Amsterdam, p 503
165. Tomoshige R, Goto T, Matsushita T, Imamura K, Chiba A, Fujita M (1999) J Mater Process Technol 85(1–3):100
166. Arkens O, Delaey L, De Tavernier J, Huybrechts B, Buekenhout L, Libouton JC (1989) Mater Res Soc Symp 133:493
167. Gur'ev DL, Gordopolov YA, Zaripov NG, Kabirov RR (2009) Combust Explos Shock Waves 45:104
168. Song I, Thadhani NN (1992) Met Trans A 23A:41
169. Mukasyan AS, White JDE (2007) Int J Self-Prop High-Temp Syn 16(3):154
170. Kimata T, Uenishi K, Ikenaga A, Kobayashi KF (2004) Sci Technol Adv Mater 5:251
171. Pascal C, Marin-Ayral RM, Tedenac JC (2001) J Mater Synth Process 9(6):375
172. Pascal C, Martin-Ayral RM, Tedenac JC, Merlet C (2003) J Mater Process Technol 135:91
173. Sytschev AE, Vadchenko SG, Kamynina OK, Sachkova NV (2009) Int J Self-Prop High-Temp Syn 18(3):213
174. Suman Das (2003) Adv Eng Mater 5(10):701
175. Li Y, Hu J, Liu Y, Guo Z, Tosto S (2009) J Mater Process Technol 209:2564
176. Zakiev SE, Kholpanov LP, Shishkovsky IV, Parkin IP, Kuznetsov MV, Morozov Y (2006) Appl Phys A 84:123
177. Shishkovsky IV, Kuznetsov MV, Morozov YG, Parkin IP (2004) J Mater Chem 14:3444
178. Masanta M, Shariff SM, Choudhury AR (2010) Surf Coat Technol 204(16–17):2527
179. Gureev DM, Petrov AL, Shishkovsky IV (199) In: Proceedings of SPIE, vol 3688. The International Society of Optical Engineering, p 237
180. Shishkovsky IV, Scherbakov VI, Morozov YG, Kuznetsov MV, Parkin IP (2008) J Therm Anal Calor 91(2):427
181. Shishkovsky I, Morozov Y, Smurov I (2009) Appl Surf Sci 255:5565
182. Chen Y, Chung DDL (1996) J Mater Sci 31:2117. doi: 10.1007/BF00356634
183. Marchi CS, Mortensen A (1998) Met Mater Trans A 29A:2819
184. Suganuma K (1993) Mater Lett 6:22
185. Yin X, Travitzky N, Greil P (2007) J Am Ceram Soc 90(7):2128
186. Giunchi G, Ripamonti G, Perini E, Cavallin T, Bassani E (2007) IEE Trans Appl Supercond 17(2):2761
187. Si-Zhou J, Xiang X, Zhao-Ke C, Peng X, Bai-Yun H (2009) Mater Des 30:3738
188. Xia H, Wang J, Jin H, Shi Z, Qiao G (2010) Mater Sci Eng A 528:283
189. Kobayashi Y, Kobashi M, Kanetake N (2008) Mater Trans 49(7):1616
190. Zhang W, Travitzky N, Greil P (2008) J Am Ceram Soc 91(9):3117